OPEN ACCESS

Original research

Lactococcus lactis HkyuLL 10 suppresses colorectal tumourigenesis and restores gut microbiota through its generated alpha-mannosidase

Anthony Chin Yang Su,[1] Xiao Ding,[1] Harry Cheuk Hay Lau ,[1] Xing Kang,[1,2] Qing Li,[1] Xueliang Wang,[1] Yali Liu,[1] Lanping Jiang,[1] Yinghong Lu,[1] Weixin Liu,[1] Yanqiang Ding,[1] Alvin Ho-Kwan Cheung,[3] Ka Fai To,[3] Jun Yu [1]

► Additional supplemental material is published online only. To view, please visit the journal online (https://doi.org/10.1136/gutjnl-2023-330835).

[1]Institute of Digestive Disease, Department of Medicine and Therapeutics, State Key Laboratory of Digestive Disease, Li Ka Shing Institute of Health Sciences, CUHK Shenzhen Research Institute, The Chinese University of Hong Kong, Hong Kong, China
[2]Lee Kong Chian School of Medicine, Nanyang Technological University, Singapore
[3]Department of Anatomical and Cellular Pathology, The Chinese University of Hong Kong, Hong Kong, China

Correspondence to
Dr Jun Yu, Department of Medicine and Therapeutics, The Chinese University of Hong Kong Faculty of Medicine, Hong Kong, Hong Kong; junyu@cuhk.edu.hk

XD, HCHL and XK are joint first authors.

Received 3 August 2023
Accepted 29 March 2024

To cite: Su ACY, Ding X, Lau HCH, *et al*. *Gut* Epub ahead of print: [*please include* Day Month Year]. doi:10.1136/gutjnl-2023-330835

ABSTRACT

Objective Probiotic *Lactococcus lactis* is known to confer health benefits to humans. Here, we aimed to investigate the role of *L. lactis* in colorectal cancer (CRC).

Design *L. lactis* abundance was evaluated in patients with CRC (n=489) and healthy individuals (n=536). *L. lactis* was isolated from healthy human stools with verification by whole genome sequencing. The effect of *L. lactis* on CRC tumourigenesis was assessed in transgenic $Apc^{Min/+}$ mice and carcinogen-induced CRC mice. Faecal microbiota was profiled by metagenomic sequencing. Candidate proteins were characterised by nano liquid chromatography-mass spectrometry. Biological function of *L. lactis* conditioned medium (*HkyuLL 10*-CM) and functional protein was studied in human CRC cells, patient-derived organoids and xenograft mice.

Results Faecal *L. lactis* was depleted in patients with CRC. A new *L. lactis* strain was isolated from human stools and nomenclated as *HkyuLL 10*. *HkyuLL 10* supplementation suppressed CRC tumourigenesis in $Apc^{Min/+}$ mice, and this tumour-suppressing effect was confirmed in mice with carcinogen-induced CRC. Microbiota profiling revealed probiotic enrichment including *Lactobacillus johnsonii* in *HkyuLL 10*-treated mice. *HkyuLL 10*-CM significantly abrogated the growth of human CRC cells and patient-derived organoids. Such protective effect was attributed to *HkyuLL 10*-secreted proteins, and we identified that α-mannosidase was the functional protein. The antitumourigenic effect of α-mannosidase was demonstrated in human CRC cells and organoids, and its supplementation significantly reduced tumour growth in xenograft mice.

Conclusion *HkyuLL 10* suppresses CRC tumourigenesis in mice through restoring gut microbiota and secreting functional protein α-mannosidase. *HkyuLL 10* administration may serve as a prophylactic measure against CRC.

WHAT IS ALREADY KNOWN ON THIS TOPIC

⇒ Depleted beneficial microbes in the gut microbiota is associated with colorectal cancer (CRC) tumourigenesis.
⇒ Probiotic supplementation is known to confer health benefits to humans.

WHAT THIS STUDY ADDS

⇒ We identified that the abundance of a probiotic species *Lactococcus lactis* is reduced in patients with CRC from three independent cohorts.
⇒ A new *L. lactis* strain, *HkyuLL 10*, was successfully isolated from healthy human stools and verified by whole genome sequencing.
⇒ *HkyuLL 10* supplementation suppressed tumourigenesis in two CRC mouse models, accompanied by alleviating gut microbial dysbiosis with enriched probiotic species.
⇒ We identified that α-mannosidase is the functional protein of *HkyuLL 10* by nano liquid chromatography-mass spectrometry.
⇒ The protective function of α-mannosidase was demonstrated in human CRC cells and patient-derived organoids, and it also markedly reduced tumour growth in CRC xenograft mice.

HOW THIS STUDY MIGHT AFFECT RESEARCH, PRACTICE OR POLICY

⇒ *HkyuLL 10* exhibits protective function against CRC tumourigenesis in mice by restoring gut dysbiosis and secreting functional protein α-mannosidase.
⇒ Supplementation of *HkyuLL 10* is a potential prophylactic measure against CRC in humans.

INTRODUCTION

Colorectal cancer (CRC) is the second leading cause of cancer-related motility and the third-most common cancer worldwide.[1] To reduce CRC burden, it is important to identify prophylactic agents to prevent its development at early stage or reduce recurrence following disease remission. It is well-known that the gut microbiota plays crucial roles in colorectal tumourigenesis. A dysregulated microbiota could disrupt intestinal homeostasis and contribute to CRC development.[2] Given its importance, modulating gut microbiota for the prevention and treatment of CRC is one of the major dogmas being investigated, and current methods of microbiota manipulation include dietary intervention, faecal microbiota transplantation and direct administration of probiotics.

Probiotics are beneficial bacteria exerting health benefits once consumed. Multiple probiotics have

been reported to exhibit inhibitory effect against CRC through releasing specific proteins or metabolites. For instance, *Streptococcus thermophilus* secretes protein β-galactosidase to inactivate the oncogenic Hippo signalling pathway,[3] whereas *Lactobacillus gallinarum* produces metabolite indole-3-lactic acid against CRC tumourigenesis in mice.[4] For humans, studies showed that ingestion of prebiotic, probiotic and symbiotic supplements are associated with significant decrease in CRC occurrence.[5] These findings therefore demonstrated the potential of probiotics as prophylactics against colorectal tumourigenesis.

Through multicohort metagenomic analysis, we previously identified the marked depletion of probiotics in patients with CRC, including *Lactococcus lactis*.[6] *L. lactis* is a Gram-positive lactic acid-producing bacterium frequently used in dairy product fermentation, and has been considered safe for human consumption. Previous study has reported that two *L. lactis* strains could be exploited as a probiotic cocktail to promote colonisation of beneficial commensals and IgA-mediated immunomodulation in human intestines.[7] Here, we investigated the role of *L. lactis* in the early prevention of CRC. We revealed the marked depletion of *L. lactis* in patients with CRC, and successfully isolated a new strain of *L. lactis* (nomenclated as '*HkyuLL 10*') from healthy human stools. *HkyuLL 10* exhibited robust antitumourigenic effect in vitro and in CRC mouse models. Through mass spectrometry characterisation, α-mannosidase (αMAN) was identified as the key protein responsible for the protection function of *HkyuLL 10*, while it could significantly inhibit tumour growth in CRC mouse xenografts.

METHODS

Bacteria isolation and culture

HkyuLL 10, a new strain of *L. lactis,* was isolated from healthy human stools. Faecal samples were first homogenised in sterilised phosphate-buffered saline (PBS) and filtered through cell strainer with a pore size of 100 µm. For selection culture, the filtered faecal solution was spread on M17 agar plate with 1% lactose. Three other strains of *L. lactis* were purchased from DSMZ (#4366, #20175, #20250; Braunschweig, Germany). *Escherichia coli* strain MG1655 (ATCC 700926, Manassas, Virginia, USA), a non-pathogenic human commensal intestinal bacterium,[8] was used as a bacterial control. Both *HkyuLL 10* and *E. coli* were cultured in brain heart infusion (BHI) broth under aerobic conditions. Bacterial conditioned medium (CM) was collected by centrifugation at 5000 rpm for 30 min and purification by filters with a pore size of 0.22 µm.

CRC tumourigenesis mouse models

Male transgenic $Apc^{Min/+}$ mice aged 6 weeks were randomly segregated to receive one of the three treatments: (1) BHI broth; (2) *E. coli* MG1655 or (3) *HkyuLL 10*. A carcinogen-induced CRC mouse model was also established. Male C57BL/6 conventional mice aged 5 weeks were intraperitoneally injected with a single dose of azoxymethane (AOM; 10 mg/kg) (Merck, Darmstadt, Germany), followed by 7-day supplementation of 1% dextran sodium sulfate (DSS; MP Biomedicals, Solon, Ohio, USA) in drinking water. Bacterial gavage was started 7 days after DSS administration. Mice were daily gavaged with 1×10^8 colony-forming unit of bacteria (*E. coli* or *HkyuLL* 10) resuspended in 100 µL of BHI broth. Mouse colonoscopy (Karl Storz Endoskope, Tuttlingen, Germany) was conducted to confirm tumour growth before sacrifice. $Apc^{Min/+}$ mice and AOM/DSS-treated mice were respectively sacrificed 12 weeks and 17 weeks after treatment, and small intestine, colon and stools were examined.

CRC tumourigenesis germ-free mouse model

Male germ-free BALB/c mice aged 8 weeks were intraperitoneally injected with a single dose of AOM (10 mg/kg), followed by three cycles of 7-day supplementation of 1% DSS in drinking water. Each cycle was separated by 7 days of resting period without DSS administration. After DSS cycles were completed, mice were randomly segregated to receive bacterial gavage (1×10^7 colony-forming unit) once per week. Mouse colonoscopy was conducted to confirm tumour growth before sacrifice. Mice were sacrificed 7 weeks after treatment, and colon was examined.

CRC xenograft mouse model

Male nude mice aged 5 weeks were subcutaneously injected with human CRC cell line HCT116 or HT29 (4×10^6 cells in 100 µL of Matrigel; Corning, Corning, New York, USA) into both left and right lower back areas (two tumours per mouse). Mice were randomly separated to receive either PBS or αMAN (1 mg/mL in PBS; #M7257, Sigma-Aldrich, St. Louis, Missouri, USA) by subcutaneous and intratumoural injection (100 µL per tumour). Treatment was carried out every 3 days along with tumour size measurement. Mice were sacrificed 2–3 weeks after treatment.

Shotgun metagenomic sequencing and analysis

Our in-house metagenomes (patient with CRC=203, healthy individual=184)[9] and two published metagenomic datasets (2019_YachidaS cohort,[10] patient with CRC=186, healthy individual=252; 2021_YangYZ cohort,[11] patient with CRC=100, healthy individual=100) were retrieved to examine the abundance of *L. lactis* in human faecal samples. Genomic DNA of mouse stools (100 mg) was extracted by PowerSoil Pro Kit (Qiagen, Hilden, Germany), and subjected to shotgun metagenomic sequencing (Illumina HiSeq 2000 platform) performed by Novogene (Beijing, China). Raw reads were checked by KneadData (V.0.12.0) to ensure that data consisted of high-quality contamination-free microbial reads. Taxa were assigned to metagenomic clean reads using k-mer-based algorithms implemented in Kraken 2 (V.2.1.2) taxonomic annotation pipeline. After rarefying to the minimal library size (6 045 977 reads), alpha (Shannon and Chao1 index) and beta diversities (principal coordinate analysis (PCoA)) were analysed using R package phyloseq (V.3.16). Dissimilarity among microbial communities was calculated by permutational multivariate analyses of variance (ANOVA) with 1000 iterations using Bray-Curtis distance. Differential species were identified by multivariate model MaAsLin2, and only taxa with relative abundance >0.01 in at least one sample were retained. Microbes with p value <0.05 and adjusted p value <0.05 (false discovery rate corrected) were considered statistically significant.

Construction of αMAN-expressing *E. coli* mutant strain

The sequence of αMAN in *HkyuLL 10* was introduced into *E. coli* MG1655 to construct a mutant strain with αMAN expression. In brief, αMAN gene from *HkyuLL 10* was amplified by PCR using αMAN-attλ primers. The insert and attλ plasmid were then ligated and introduced to *E. coli* DH5α, followed by inoculation on Lysogeny brot (LB) agar with ampicillin at 37°C overnight. After incubation, colonies were selected and the introduction of plasmid was confirmed by PCR using αMAN-cx primers. The selected plasmid was then transformed into *E. coli* MG1655 by electroporation. Successful insertion of αMAN sequence was validated by PCR using MG1655attλ primers. Primers used for bacterial engineering are listed in online supplemental table 1.

Statistical analyses

All results are shown as mean±SD. Mann-Whitney U test was used to compare the difference in numerical variables between two groups unless specified. One-way ANOVA was used to compare the difference in numerical variables among three groups. Repeated measures two-way ANOVA was used to compare different timepoints or stages between two groups. All statistical tests were performed using GraphPad Prism (V.9.0) or R language. Two-tailed p value <0.05 was considered statistically significant.

Additional methods are provided in online supplemental information.

RESULTS

L. lactis is depleted in stools of patients with CRC

We first analysed the relative abundance of *L. lactis* in our in-house faecal metagenomic cohort.[9] The abundance of *L. lactis* was significantly depleted in faecal samples of patients with CRC as compared with healthy individuals (p<0.0001; figure 1A). For validation, we retrieved two published faecal metagenomic datasets and confirmed the marked depletion of *L. lactis* in patients with CRC from 2019_ YachidaS cohort[10] (p<0.01) and 2021_YangYZ cohort[11] (p<0.0001), compared with healthy individuals.

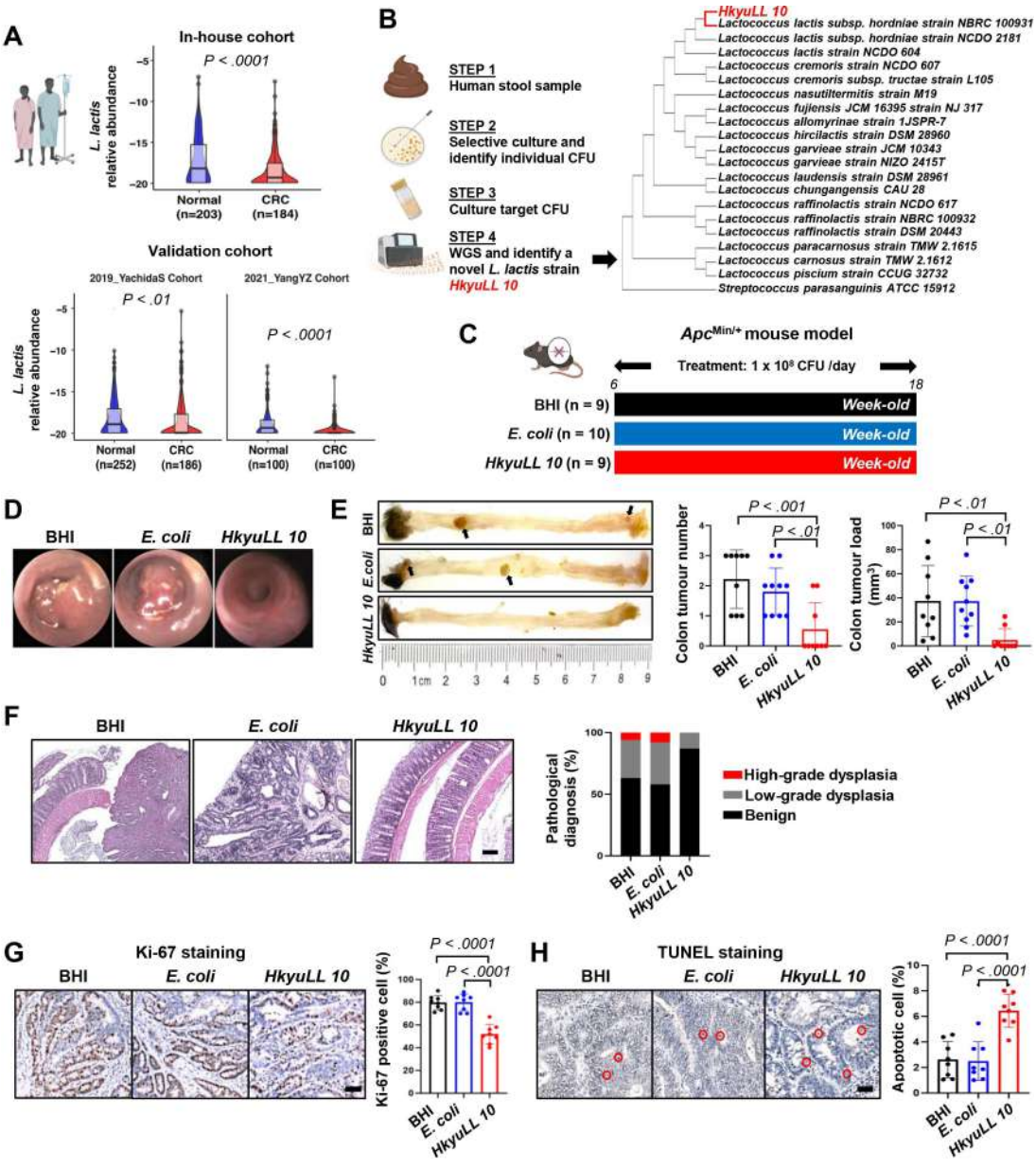

Figure 1 *HkyuLL 10* protects against CRC tumourigenesis in *Apc*$^{Min/+}$ mice. (A) Faecal abundance of *Lactococcus lactis* in patients with CRC and healthy individuals from an in-house cohort and two published metagenomic datasets. (B) Isolation of a novel *L. lactis* strain and phylogenetic tree of *HkyuLL 10*. (C) Experimental schematic of *Apc*$^{Min/+}$ mice with daily supplementation of *HkyuLL 10* or control (BHI broth or *Escherichia coli*). (D) Representative images of colonoscopy. (E) Colon morphology and tumour parameters, with black arrows indicating the visible tumours. (F) Representative colon H&E images and scoring of dysplasia. Scale bar=100 µm. (G, H) Representative images and scoring of Ki-67 staining (G) or TUNEL staining (H) in tumour tissues. Positively stained cells are circled in red. Scale bar=50 µm. BHI, brain heart infusion; CFU, colony-forming unit; CRC, colorectal cancer; WGS, whole genome sequencing.

A new *L. lactis* strain *HkyuLL 10* protects against CRC tumourigenesis in *Apc*$^{Min/+}$ mice

We successfully isolated *L. lactis* from faecal samples of healthy human individuals. Through whole genome sequencing, we identified that our isolated strain had a close phylogenetic relationship to *L. lactis* subspecies Hordniae strain NBRC 100931 but with different genomic sequence. The whole genome sequences of *HkyuLL 10* and *L. lactis* Hordniae strain NBRC 100931 are provided in online supplemental data 1 and 2, respectively. Hence, we confirmed our discovery of a new *L. lactis* strain and nomenclated as '*HkyuLL 10*' (figure 1B).

We evaluated the effect of *HkyuLL 10* in *Apc*$^{Min/+}$ mice, a transgenic mouse model of intestinal tumourigenesis, with daily gavage of BHI broth, *E. coli* or *HkyuLL 10* (figure 1C). Visually smaller tumours were observed in *HkyuLL 10*-treated mice than control mice treated with BHI or *E. coli* under colonoscopy (figure 1D). After 12 weeks of treatment, mice were sacrificed and significant reduction in tumour number and tumour load was observed in the colon (figure 1E) and small intestine (online supplemental figure 3) of *HkyuLL 10*-treated mice, compared with control mice. Histological assessment showed that *HkyuLL 10*-treated mice had a lower percentage of low-grade dysplasia as compared with the two control groups (figure 1F). *HkyuLL 10* supplementation also markedly reduced the amount of Ki-67 positive proliferating cells (figure 1G) and increased apoptotic cells (figure 1H) in tumour tissues of gavaged mice.

HkyuLL 10 protects conventional mice from carcinogen-induced CRC tumourigenesis

We then tested the tumour-suppressing effect of *HkyuLL 10* in another CRC tumourigenesis mouse model chemically induced by AOM/DSS, with daily gavage of BHI, *E. coli* or *HkyuLL 10* (figure 2A). Visually smaller tumours were observed in *HkyuLL 10*-treated mice than control mice treated with BHI or *E. coli* under colonoscopy (figure 2B). After 17 weeks of treatment, mice were sacrificed and we observed significant reduction in tumour number and tumour load in the colon of *HkyuLL 10*-treated mice (figure 2C). Histological assessment showed that *HkyuLL 10*-treated mice had a lower percentage of low-grade dysplasia as compared with the two control groups (figure 2D). *HkyuLL 10* supplementation also significantly

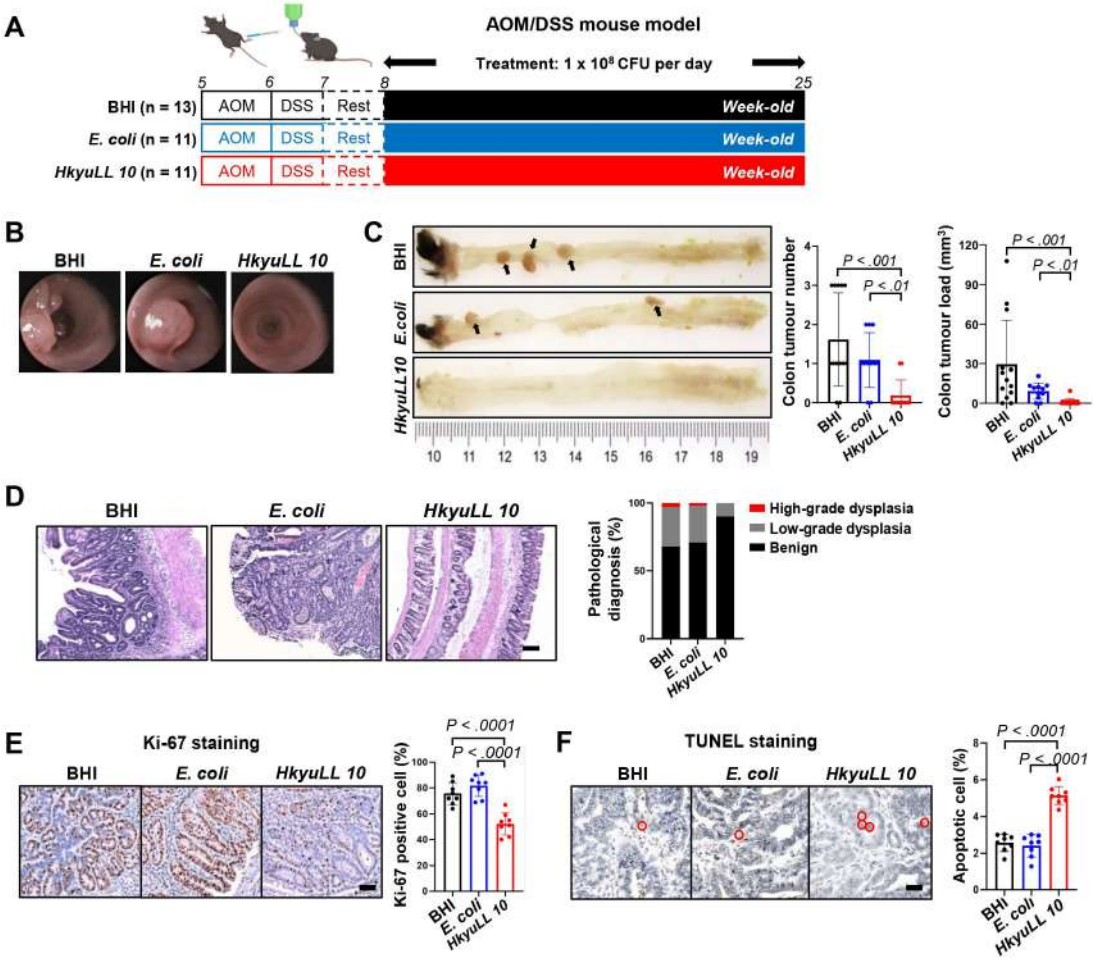

Figure 2 *HkyuLL 10* protects conventional mice from carcinogen-induced CRC tumourigenesis. (A) Experimental schematic of AOM/DSS-treated conventional mice with daily supplementation of *HkyuLL 10* or control (BHI broth or *Escherichia coli*). (B) Representative images of colonoscopy. (C) Colon morphology and tumour parameters, with black arrows indicating the visible tumours. (D) Representative colon H&E images and scoring of dysplasia. Scale bar=100 µm. (E, F) Representative images and scoring of Ki-67 staining (E) or TUNEL staining (F) in tumour tissues. Positively stained cells are circled in red. Scale bar=50 µm. AOM, azoxymethane; BHI, brain heart infusion; CFU, colony-forming unit; CRC, colorectal cancer; DSS, dextran sodium sulfate.

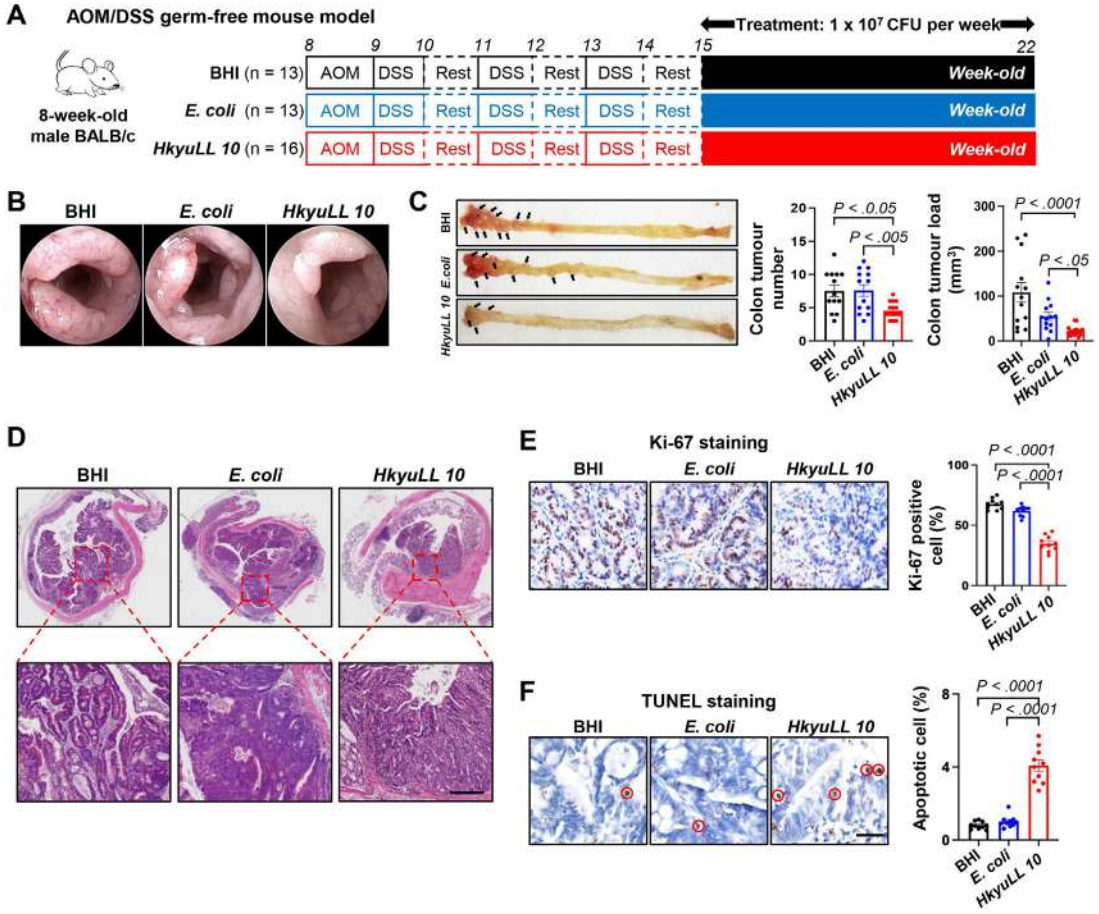

Figure 3 *HkyuLL 10* protects germ-free mice from carcinogen-induced CRC tumourigenesis. (A) Experimental schematic of AOM/DSS-treated germ-free mice with weekly supplementation of *HkyuLL 10* or control (BHI broth or *Escherichia coli*). (B) Representative image of colonoscopy. (C) Colon morphology and tumour parameters, with black arrows indicating the visible tumours. (D) Representative colon H&E images. Scale bar=100 µm. (E, F) Representative images and scoring of Ki-67 staining (E) or TUNEL staining (F) in tumour tissues. Positively stained cells are circled in red. Scale bar=50 µm. AOM, azoxymethane; BHI, brain heart infusion; CFU, colony-forming unit; CRC, colorectal cancer; DSS, dextran sodium sulfate.

decreased Ki-67 positive proliferating cells (figure 2E) and increased apoptotic cells (figure 2F) in tumour tissues of gavaged mice. Together, the consistent findings between two mouse models indicated the protective role of *HkyuLL 10* against CRC tumourigenesis in mice.

HkyuLL 10 protects germ-free mice from carcinogen-induced CRC tumourigenesis

To evaluate the sole beneficial effect of *HkyuLL 10*, we supplemented BHI, *E. coli* or *HkyuLL 10* to germ-free mice with AOM/DSS-induced CRC tumourigenesis (figure 3A). Visually smaller tumours were observed in *HkyuLL 10*-treated mice than control mice treated with BHI or *E. coli* under colonoscopy (figure 3B). After 7 weeks of treatment, mice were sacrificed and we found that *HkyuLL 10* significantly decreased tumour number and tumour load in the colon of gavaged mice, compared with control (figure 3C). Histological assessment confirmed the occurrence of colon cancer in mice (figure 3D). Significantly decreased Ki-67 positive proliferating cells (figure 3E) and increased apoptotic cells (figure 3F) were observed in tumour tissues of *HkyuLL 10*-treated mice, compared with control. Hence, these findings demonstrated that *HkyuLL 10* alone is adequate to suppress CRC tumourigenesis in mice with a depleted microbiota.

HkyuLL 10 modulates gut microbiota with enriched probiotics in CRC mice

Since probiotics could confer benefits against colorectal tumourigenesis by modulating microbiota, we elucidated the impact of *HkyuLL 10* on the gut microbiota by performing metagenomic sequencing on faecal samples of $Apc^{Min/+}$ mice. β-Diversity analysis by PCoA showed that the microbial community in *HkyuLL 10*-treated mice was distinctively separated from the two control groups (figure 4A), implying that *HkyuLL 10* could alter the composition of gut microbiota. A significant shift of microbial species was also observed in *HkyuLL 10*-treated mice, particularly including the enrichment of known probiotics such as *Propionibacterium freudenreichii*, *Akkermansia muciniphila*, *L. johnsonii*, *Lactobacillus intestinalis* and *Limosilactobacillus reuteri* (figure 4B).

Metagenomic sequencing was also conducted on faecal samples of mice with AOM/DSS-induced CRC, and β-diversity analysis by PCoA showed that the microbial community in *HkyuLL 10*-treated mice was distinct from the two control groups (figure 4C). Similar to $Apc^{Min/+}$ mice, *HkyuLL 10* supplementation greatly altered the gut microbiota with enriched probiotics including *L. reuteri*, *L. intestinalis* and *L. johnsonii* in gavaged AOM/DSS-treated mice

(figure 4D). These findings therefore implied that *HkyuLL 10* could elevate the abundance of commensal probiotics against CRC tumourigenesis in mice. In addition, differential analysis identified the enrichment of *HkyuLL 10* in both gavaged *Apc*$^{Min/+}$ (figure 4B) and AOM/DSS-treated mice (figure 4D). For further verification, PCR detection and Sanger sequencing were performed using custom-designed primers for *HkyuLL 10* and *E. coli* MG1655 (online supplemental table 2). The results confirmed the specific enrichment of *HkyuLL 10* or *E. coli* in gavaged mice, respectively (online supplemental figure 2).

HkyuLL 10 inhibits growth of CRC cells and patient-derived organoids

To understand the antitumourigenic mechanism of *HkyuLL 10*, we treated two human CRC cell lines (HCT116, HT29) with bacterial CM. The *HkyuLL 10*-CM at 2.5% concentration was sufficient to inhibit the viability of HCT116 cells, compared with broth control and the CM of *E. coli* (EC-CM) with the same concentration ($p<0.0001$; figure 5A). In comparison, *HkyuLL 10*-CM at 5% concentration was required to exhibit a suppressive effect on HT29 cells ($p<0.0001$; figure 5B). Meanwhile, 5% *HkyuLL 10*-CM posed no effect on the growth of human normal colon epithelial cell line NCM460 (figure 5C), suggesting that its inhibitory function was specific to CRC cells. The proportion of Ki-67-positive proliferating cells was also significantly reduced by 5% *HkyuLL 10*-CM in HCT116 (figure 5D) and HT29 (figure 5E) cells, compared with the two control groups. Consistently, the protein expression of proliferation marker proliferating cell nuclear antigen (PCNA) was downregulated in both CRC cell lines after *HkyuLL 10*-CM treatment (figure 5F). Moreover, we treated tumour organoids derived from two patients with CRC with 5% *HkyuLL 10*-CM, and observed a significant decrease in the growth of organoids as compared with broth control and EC-CM (figure 5G). Through bacteria-cell attachment assay, we further showed that *HkyuLL 10* could attach to HCT116 and HT29 cells (both $p<0.0001$; figure 5H). Direct co-culture with *HkyuLL 10* also suppressed the viability of HCT116 and HT29 cells, with no effect on normal NCM460 cells (online supplemental figure 3A,B). In addition, similar to *HkyuLL 10*-CM, the CM of three other *L. lactis* strains also significantly inhibited the viability of CRC cells, but not normal colon epithelial cells (online supplemental figure 3C,D), confirming the protective function of *L. lactis* in CRC.

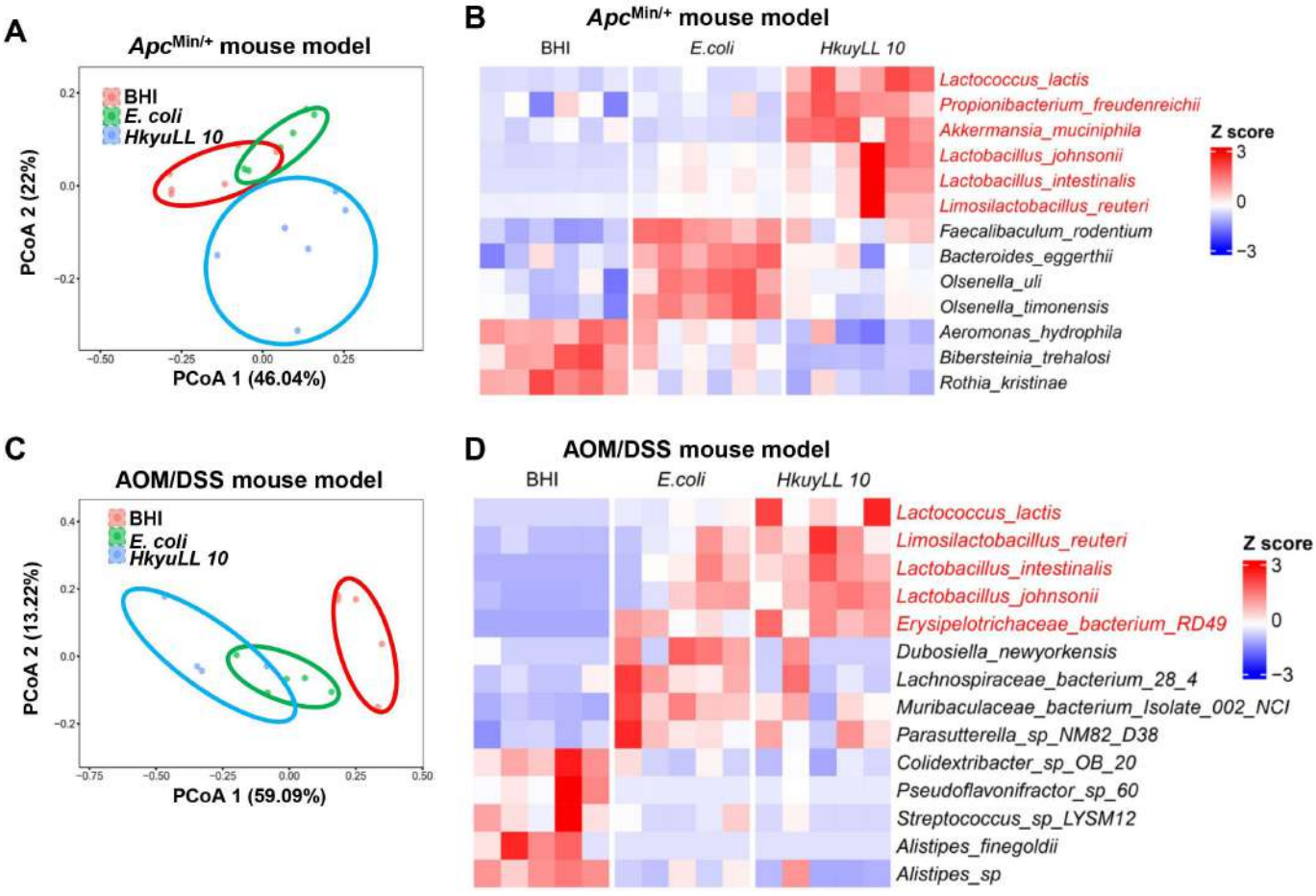

Figure 4 *HkyuLL 10* modulates gut microbiota with enriched probiotics in CRC mice. (A) Beta-diversity by PCoA based on Bray-Curtis dissimilarity matrix in faecal samples of *Apc*$^{Min/+}$ mice. (B) Heatmap of differential bacterial species ($p<0.05$) in *Apc*$^{Min/+}$ mice, compared with broth control and *Escherichia coli* bacterial control groups. (C) Beta-diversity by PCoA in faecal samples of AOM/DSS-treated mice. (D) Heatmap of differential bacterial species in AOM-DSS-treated mice. AOM, azoxymethane; BHI, brain heart infusion; CRC, colorectal cancer; DSS, dextran sodium sulfate; PCoA, principal coordinate analysis.

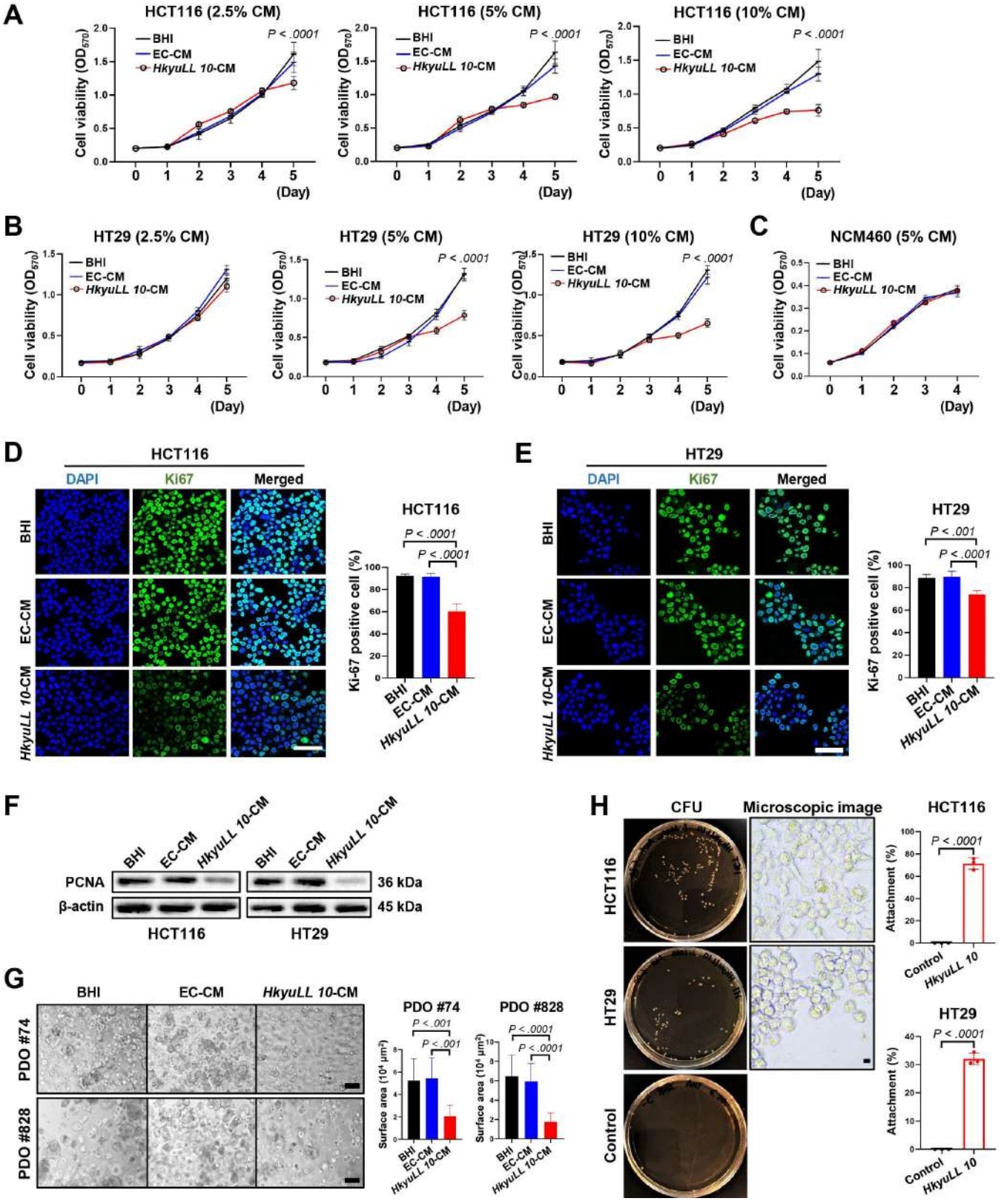

Figure 5 *HkyuLL 10* inhibits growth of CRC cells and patient-derived organoids. (A, B) Cell viability at OD_{570} of human CRC cell line HCT116 (A) or HT29 (B) under treatment of bacterial conditioned medium with different concentrations. (C) Cell viability at OD_{570} of human normal colon epithelial cell line NCM460 under treatment of 5% bacterial conditioned medium. (D, E) Representative images of Ki-67 immunofluorescent staining of HCT116 (D) or HT29 (E) cells. Scale bar=50 µm. (F) Protein expression of proliferation marker PCNA in CRC cells. (G) Representative images and size of tumour organoids derived from two patients with CRC under treatment of 5% bacterial conditioned medium. Scale bar=200 µm. (H) Macroscopic and microscopic images of *HkyuLL 10* attachment to CRC cells. Scale bar=200 µm. BHI, brain heart infusion; CFU, colony-forming unit; CM, conditioned medium; CRC, colorectal cancer; DAPI, 4',6-diamidino-2-phenylindole; EC-CM, CM of *Escherichia coli*; OD, optical density; PDO, patient-derived organoid.

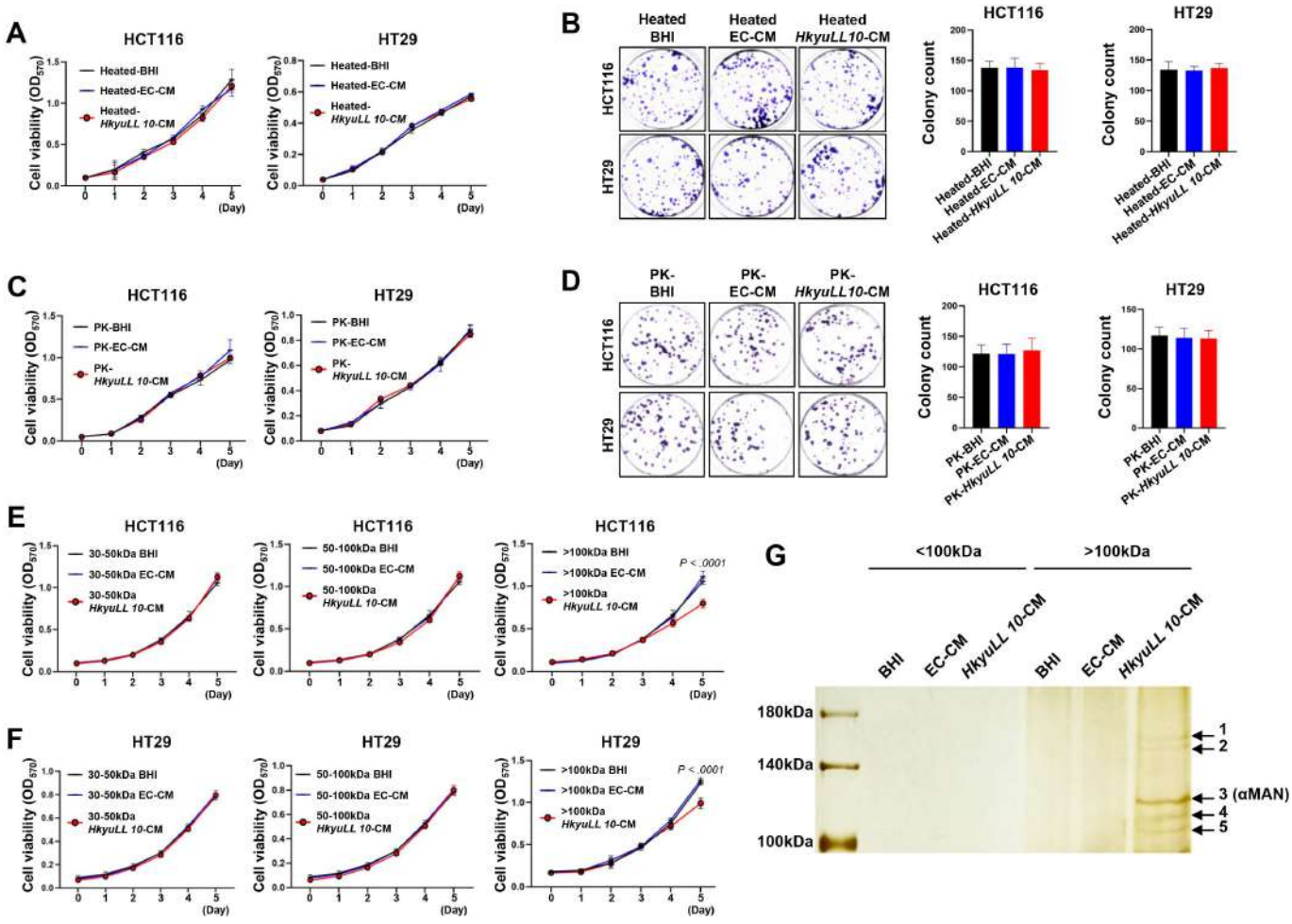

Figure 6 *HkyuLL 10* produces antitumourigenic proteins with a molecular weight of >100 kDa. (A, B) Cell viability at OD_{570} (A) and colony formation (B) of CRC cells under treatment of heat-inactivated bacterial conditioned medium. (C, D) Cell viability at OD_{570} (C) and colony formation (D) of CRC cells under treatment of PK-treated bacterial conditioned medium. (E, F) Cell viability at OD_{570} of HCT116 (E) or HT29 (F) cells under treatment of bacterial conditioned medium with different molecular fractions. (G) Image of silver staining on bacterial conditioned medium, with arrows indicating five protein bands visible only in *HkyuLL 10*-CM >100 kDa. αMAN, α-mannosidase; BHI, brain heart infusion; CM, conditioned medium; CRC, colorectal cancer; EC-CM, CM of *Escherichia coli*; OD, optical density; PK, proteinase K.

HkyuLL 10 produces antitumourigenic proteins with a molecular weight of >100 kDa

We next investigated molecules responsible for the antitumourigenic function of *HkyuLL 10*-CM. Bacteria can secrete various molecules including proteins and metabolites. Our results showed that the inhibitory effect of *HkyuLL 10*-CM on both HCT116 and HT29 CRC cell lines was completely abolished after heat inactivation (figure 6A). Heat-inactivated *HkyuLL 10*-CM also failed to restrain colony formation of CRC cells, as evidenced by the similar number of cell colonies observed among all groups (figure 6B). For validation, we treated *HkyuLL 10*-CM with proteinase K. Indeed, no inhibitory effect was demonstrated by proteinase K-treated *HkyuLL 10*-CM in HCT116 and HT29 cells, compared with proteinase K-treated broth control and EC-CM (figure 6C). Consistently, there was no difference in the number of cell colonies among all groups after proteinase K treatment (figure 6D). Hence, these results implied that the antitumourigenic molecules produced by *HkyuLL 10* are proteins.

To characterise the functional proteins, bacterial CM was separated into different fractions based on their molecular weight (30–50 kDa, 50–100 kDa, >100 kDa). We identified that only *HkyuLL 10*-CM with >100 kDa exhibited significant inhibitory effect on HCT116 cells ($p<0.0001$), while *HkyuLL 10*-CM with 30–50 kDa or 50–100 kDa had no impacts (figure 6E). Similar results were observed in HT29 cell line, where only *HkyuLL 10*-CM with >100 kDa could inhibit its viability ($p<0.0001$; figure 6F). Silver staining was therefore conducted on *HkyuLL 10*-CM with >100 kDa, and five distinct proteins bands with a molecular weight of >100 kDa were observed (figure 6G). Nano LC-MS analysis was then performed to characterise these five candidate proteins (online supplemental table 3), and αMAN was selected as the functional protein of *HkyuLL 10*. Through whole genome sequencing, the αMAN-encoding sequence in *HkyuLL 10* genome was identified (online supplemental table 4).

α-Mannosidase inhibits growth of CRC cells and patient-derived organoids

The role of αMAN was tested in human CRC cells. We revealed that αMAN had similar activity in cell culture medium and bacteria culture broth (online supplemental figure 4A). αMAN significantly inhibited the viability of HCT116 ($p<0.01$) and HT29 ($p<0.01$) CRC cells in a concentration-dependent manner,

whereas a much higher concentration of αMAN was required to reduce the viability of normal NCM460 cells (figure 7A and online supplemental figure 4B). αMAN treatment also markedly restrained the colony formation of CRC cells, compared with control ($p<0.01$; figure 7B). Moreover, a significant reduction in the size of CRC patient-derived organoids was observed after αMAN treatment ($p<0.001$; figure 7C). To confirm the functional role of αMAN, we introduced the sequence of αMAN into *E. coli* to construct a mutant strain with αMAN expression (online supplemental figure 4C). The CM of αMAN-expressing *E. coli* had similar inhibitory effect as *HkyuLL 10*-CM by suppressing the viability (figure 7D) and colony formation (online supplemental figure 4D) of HCT116 and HT29 cells. The growth of CRC patient-derived organoids was also significantly reduced by the CM of αMAN-expressing *E. coli* (figure 7E).

α-Mannosidase suppresses tumour growth in CRC xenograft mice

We next validated the effect of αMAN in CRC xenograft mouse models bearing HCT116 tumours. Consistent with in vitro findings, αMAN exhibited robust antitumourigenic effect in HCT116 xenografts, as evidenced by the significant decrease in tumour growth compared with control mice receiving PBS ($p<0.05$; figure 7F). On sacrifice, macroscopic examination revealed the marked reduction in tumour volume ($p<0.01$) and tumour weight ($p<0.001$) in HCT116 xenografts treated with αMAN (figure 7F). Significantly decreased Ki-67-positive proliferating cells ($p<0.001$; figure 7G) and increased apoptotic cells ($p<0.001$; figure 7H) were also observed in HCT116 tumours of αMAN-treated xenografts, compared with control mice.

For validation, another CRC xenograft mouse model was established by injecting HT29 CRC cells. As expected, αMAN significantly suppressed tumour growth in these HT29 xenografts, compared with control mice receiving PBS ($p<0.0001$; figure 7I). On sacrifice, we observed the marked decrease in tumour volume and tumour weight in HT29 xenografts treated with αMAN (both $p<0.001$; figure 7I). Significantly decreased Ki-67-positive proliferating cells ($p<0.001$; figure 7J) and increased apoptotic cells ($p<0.001$; figure 7K) were also observed in HT29 tumours of αMAN-treated xenografts, compared with control mice. Together, our consistent in vitro and in vivo findings illustrated that *HkyuLL 10* secretes protein αMAN to protect against CRC.

DISCUSSION

In this study, we investigated the protective role of *L. lactis* against colorectal tumourigenesis. We first confirmed the faecal depletion of *L. lactis* in our in-house cohort and published metagenomic datasets of patients with CRC (figure 1). This result prompted us to hypothesise that *L. lactis* may play a pivotal role against CRC. Metagenomic analysis also suggested the presence of *L. lactis* in the gut microbiota of healthy individuals. Indeed, a strain of *L. lactis* was successfully isolated from healthy human stools. Through whole genome sequencing, we discovered that its genome is closely related but not completely identical to *L. lactis* subspecies Hordniae strain NBRC 100931, thus implying our identification of a new *L. lactis* strain (nomenclated as '*HkyuLL 10*').

Here, we for the first time showed that *L. lactis* supplementation is sufficient to alleviate CRC tumourigenesis in mice. By supplementing *HkyuLL 10* to mice with transgenic or carcinogen-induced CRC (figure 2), we observed that this novel *L. lactis* strain consistently abrogates CRC tumourigenesis in these mouse models. In general, probiotic supplementation is known to benefit human patients by alleviating and improving GI conditions such as diarrhoea and infection.[12] Numerous preclinical studies also reported the marked inhibition of CRC by probiotics.[3 4 13] For example, oral administration of *Lactobacillus fermentum* ZS40 was capable of mitigating intestinal inflammation and tumourigenesis in AOM/DSS-treated mice.[14] Of note, *HkyuLL 10* was able to suppress CRC tumourigenesis in germ-free mice (figure 3), indicating that *HkyuLL 10* alone is sufficient to confer protective effect in microbiota-depleted mice. Collectively, these findings implied the promising prophylactic potential of *L. lactis* against CRC, as it could exhibit antitumourigenic function in a dysregulated microbiota, which frequently occurred in patients with CRC.[15]

Through faecal metagenomic sequencing, we identified that *HkyuLL 10* could modulate the gut microbiota in CRC mice (figure 4). It is necessary for the gut microbiota to maintain a preferrable composition in the human body, whereas its alteration or dysregulation can affect various physiological functions including host immune response, digestion, metabolism and intestinal permeability.[16] In particular, the balance of gut microbiota is substantially disrupted in colorectal tumourigenesis, resulting in the occurrence of microbial dysbiosis.[15] Here, we found that *HkyuLL 10* significantly increases the abundance of well-characterised commensal probiotics such as *L. johnsonii* and *L. intestinalis* in gavaged mice. Previous studies reported that the administration of these *Lactobacilli* could facilitate the reconstruction of a balanced microbiota with improved intestinal integrity in mice.[17–19] Introducing a probiotic mixture containing six *Bifidobacteria* and *Lactobacillus* strains to postsurgery patients also lead to a significant reduction in pro-inflammatory cytokines and restoration in the intestinal microenvironment.[20] Hence, these findings indicated that *HkyuLL 10* suppresses CRC tumourigenesis, at least in part, through modulating and renovating the gut microbiota back to healthy and balanced conditions.

The results of in vitro biofunctional assays illustrated that the tumour-suppressing effect of *HkyuLL 10* is attributed to its secreted proteins (figure 5). Subsequent characterisation by mass spectrometry identified that αMAN is the key functional component of *HkyuLL 10* (figure 6). Probiotics produce different kinds of molecules including proteins and metabolites to confer health benefits,[3 21] both of which could be used for tumour cell targeting.[22] Here, we illustrated the antitumourigenic function of αMAN against the growth of CRC cells and patient-derived organoids, as well as subcutaneous tumour formation in xenograft mice (figure 7). αMAN is an enzyme expressed in the endoplasmic reticulum and Golgi apparatus of human cells for the processing and catabolism of *N*-linked glycans.[23] Some gut commensal bacteria (eg, *Bacteroides thetaiotaomicron, Enterococcus faecalis, Neobacillus novalis*) also express αMAN to modulate or degrade yeast α-mannan and mannose-rich glycans.[24–26] To ascertain the role of bacterial αMAN, we constructed a strain of *E. coli* that expressed the sequence of αMAN in *HkyuLL 10*. This mutant *E. coli* significantly inhibited the growth and proliferation of CRC cells and patient-derived organoids, thus confirming the tumour-suppressing function of *HkyuLL 10*-secreted αMAN. In general, *N*-glycans are closely associated with CRC as they can promote tumour growth, oncogenic signalling and metastasis.[27] Several *N*-glycans were also identified as potential biomarkers of CRC.[28 29] Given its ability to catabolise *N*-glycans, it is possible that αMAN degrades oncogenic *N*-glycans to protect against CRC or other cancers. For instance, αMAN could attenuate prostatic tumourigenesis by

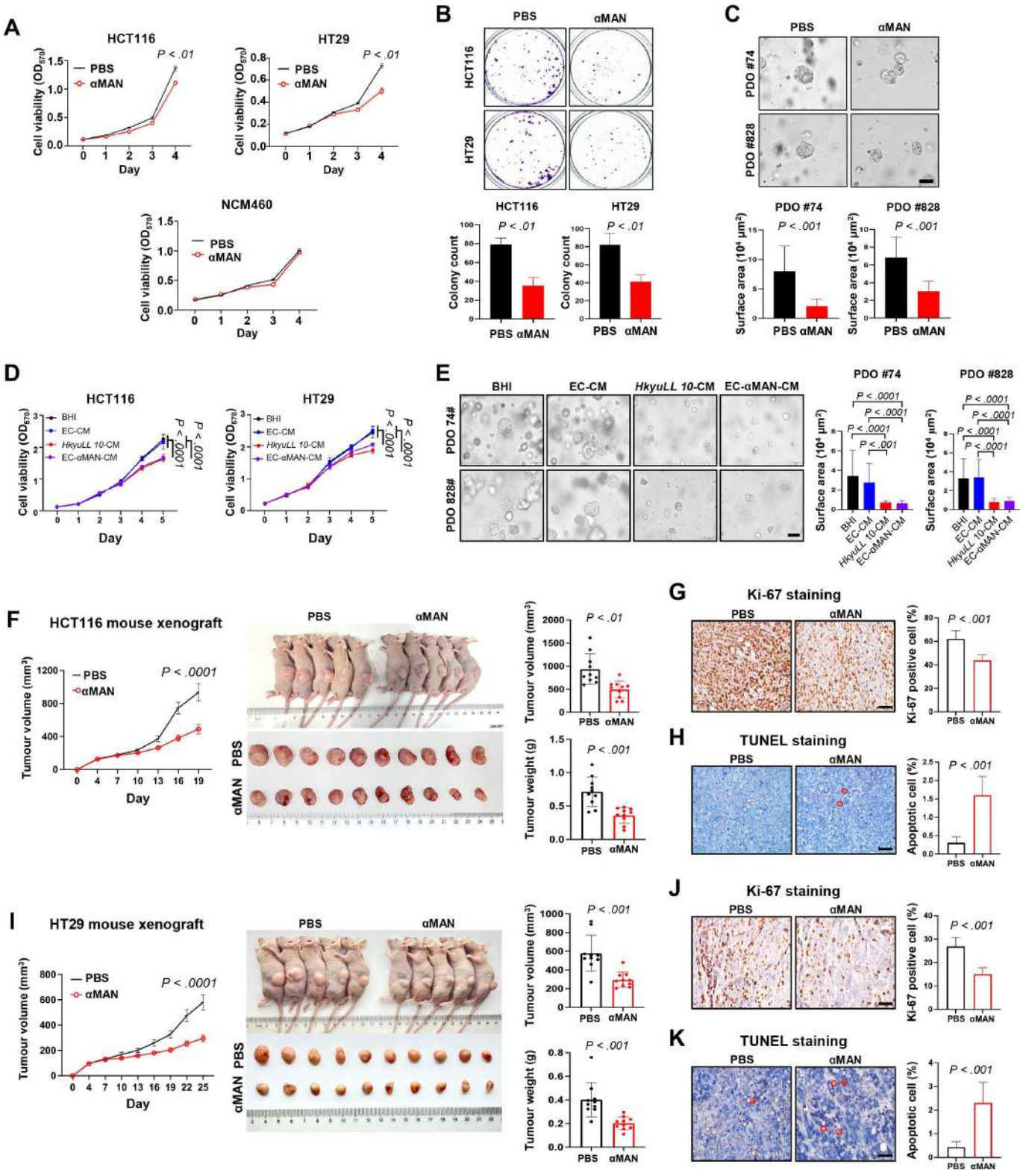

Figure 7 αMAN inhibits growth of CRC cells, patient-derived organoids and xenograft mice. (A) Cell viability at OD_{570} of human CRC cells (HCT116, HT29) and normal colon epithelial cells (NCM460) under treatment of αMAN (10 ng/mL). (B) Colony formation of CRC cells under treatment of αMAN. (C) Representative images and size of tumour organoids derived from two patients with CRC under treatment of αMAN. Scale bar=100 μm. (D) Cell viability at OD_{570} of CRC cells under treatment of 5% bacterial conditioned medium (>100 kDa). (E) Representative images and size of CRC patient-derived organoids under treatment of 5% bacterial conditioned medium (>100 kDa). (F) Tumour parameters of CRC xenograft mice bearing HCT116 tumours. (G, H) Representative images and scoring of Ki-67 staining (G) or TUNEL staining (H) in HCT116 tumours. Positively stained cells are circled in red. Scale bar=50 μm. (I) Tumour parameters of CRC xenograft mice bearing HT29 tumours. (J, K) Representative images and scoring of Ki-67 staining (J) or TUNEL staining (K) in HT29 tumours. αMAN, α-mannosidase; BHI, brain heart infusion; CRC, colorectal cancer; EC-αMAN-CM, αMAN-expressing *Escherichia coli* conditioned medium; OD, optical density; PBS, phosphate-buffered saline; PDO, patient-derived organoid.

negatively regulating the oncogenic PTEN pathway.[30] Notably, it is unlikely that αMAN alone is adequate to confer tumour-suppressing effect, as glycan degradation requires a variety of enzymes such as glucosidases, GlcNAc transferase and different members of mannosidases.[31] Further investigation is suggested to decipher the role of other microbes-derived enzymes involved in glycan degradation in CRC in the future.

In conclusion, our research is a pioneering study which illustrates the complete adoption and effectiveness of the novel *L. lactis* strain *HkyuLL 10* on CRC in multiple mouse models. *HkyuLL 10* suppressed CRC tumourigenesis in mice by enriching gut commensal probiotics and secreting αMAN. The antitumourigenic function of αMAN was verified both in vitro and in vivo. Overall, our findings indicated that *HkyuLL 10* administration is a potential prophylactic measure against colorectal tumourigenesis. Extensive research is imperative to ascertain the effect of *HkyuLL 10* and evaluate whether its combination with other well-characterised probiotics could synergistically contribute to CRC prevention in humans.

Contributors ACYS designed the study, performed the experiments and drafted the manuscript. XD, HCHL, XK and QL performed the experiments and revised the manuscript. XW, YLiu and LJ performed the experiments. YLu, WL and YD conducted bioinformatic analyses. AH-KC and KFT performed histological examination. JY designed and supervised the study and revised the manuscript. JY is the guarantor of this study.

Funding This project was supported by Research Talent Hub-Innovation and Technology Fund Hong Kong (ITS/177/21FP); RGC Research Impact Fund Hong Kong (R4032-21F); Shenzhen-Hong Kong-Macao Science and Technology Programme (Category C) Shenzhen (SGDX20210823103535016) and The Kingboard Precision Oncology Programme, CUHK.

Competing interests None declared.

Patient and public involvement Patients and/or the public were not involved in the design, or conduct, or reporting, or dissemination plans of this research.

Patient consent for publication Not applicable.

Ethics approval All animal studies were performed in accordance with guidelines approved by the Animal Experimentation Ethics Committee of The Chinese University of Hong Kong; and the Laboratory Animal Management and Use Committee of Shenzhen Jingtuo Biotechnology for germ-free mice.

Provenance and peer review Not commissioned; externally peer reviewed.

Data availability statement All data relevant to the study are included in the article or uploaded as supplementary information.

ORCID iDs
Harry Cheuk Hay Lau http://orcid.org/0000-0003-3581-2909
Jun Yu http://orcid.org/0000-0001-5008-2153

REFERENCES

1 Siegel RL, Miller KD, Fuchs HE, *et al*. Cancer statistics, 2022. *CA Cancer J Clin* 2022;72:7–33.
2 Dalal N, Jalandra R, Bayal N, *et al*. Gut Microbiota-derived metabolites in CRC progression and causation. *J Cancer Res Clin Oncol* 2021;147:3141–55.
3 Li Q, Hu W, Liu W-X, *et al*. *Streptococcus thermophilus* inhibits colorectal tumorigenesis through Secreting beta-Galactosidase. *Gastroenterology* 2021;160:e14:1179–1193..
4 Sugimura N, Li Q, Chu ESH, *et al*. *Lactobacillus gallinarum* modulates the gut Microbiota and produces anti-cancer metabolites to protect against colorectal Tumourigenesis. *Gut* 2021;71:2011–21.
5 Kim CE, Yoon LS, Michels KB, *et al*. The impact of Prebiotic, Probiotic, and Synbiotic supplements and yogurt consumption on the risk of colorectal Neoplasia among adults: A systematic review. *Nutrients* 2022;14:4937.
6 Dai Z, Coker OO, Nakatsu G, *et al*. Multi-cohort analysis of colorectal cancer Metagenome identified altered bacteria across populations and universal bacterial markers. *Microbiome* 2018;6:70.
7 Bandyopadhyay B, Das S, Mitra PK, *et al*. Characterization of two new strains of Lactococcus Lactis for their Probiotic efficacy over commercial Synbiotics consortia. *Braz J Microbiol* 2022;53:903–20.
8 Touchon M, Hoede C, Tenaillon O, *et al*. Organised genome Dynamics in the Escherichia coli species results in highly diverse adaptive paths. *PLoS Genet* 2009;5:e1000344.
9 Yu J, Feng Q, Wong SH, *et al*. Metagenomic analysis of Faecal Microbiome as a tool towards targeted non-invasive biomarkers for colorectal cancer. *Gut* 2017;66:70–8.
10 Yachida S, Mizutani S, Shiroma H, *et al*. Metagenomic and Metabolomic analyses reveal distinct stage-specific phenotypes of the gut Microbiota in colorectal cancer. *Nat Med* 2019;25:968–76.
11 Yang Y, Du L, Shi D, *et al*. Dysbiosis of human gut Microbiome in young-onset colorectal cancer. *Nat Commun* 2021;12.
12 Sałański P, Kowalczyk M, Bardowski JK, *et al*. Health-promoting nature of Lactococcus Lactis Ibb109 and Lactococcus Lactis Ibb417 strains exhibiting proliferation inhibition and stimulation of Interleukin-18 expression in colorectal cancer cells. *Front Microbiol* 2022;13:822912.
13 Kang X, Liu C, Ding Y, *et al*. Roseburia Intestinalis generated butyrate BOOSTS anti-PD-1 efficacy in colorectal cancer by activating cytotoxic Cd8(+) T cells. *Gut* 2023;72:2112–22.
14 Chen Z, Yi L, Pan Y, *et al*. *Lactobacillus fermentum* Zs40 ameliorates inflammation in mice with ulcerative colitis induced by dextran sulfate sodium. *Front Pharmacol* 2021;12:700217.
15 Wong SH, Yu J. Gut Microbiota in colorectal cancer: mechanisms of action and clinical applications. *Nat Rev Gastroenterol Hepatol* 2019;16:690–704.
16 Gomaa EZ. Human gut Microbiota/Microbiome in health and diseases: a review. *Antonie Van Leeuwenhoek* 2020;113:2019–40.
17 Sun N, Ni X, Wang H, *et al*. Probiotic Lactobacillus Johnsonii Bs15 prevents memory dysfunction induced by chronic high-fluorine intake through Modulating intestinal environment and improving gut development. *Probiotics Antimicrob Proteins* 2020;12:1420–38.
18 Lim EY, Song E-J, Kim JG, *et al*. Lactobacillus Intestinalis Yt2 restores the gut Microbiota and improves menopausal symptoms in ovariectomized rats. *Benef Microbes* 2021;12:503–16.
19 Han S, Zheng H, Han F, *et al*. Lactobacillus Johnsonii 6084 alleviated sepsis-induced organ injury by Modulating gut Microbiota. *Food Sci Nutr* 2022;10:3931–41.
20 Zaharuddin L, Mokhtar NM, Muhammad Nawawi KN, *et al*. A randomized double-blind placebo-controlled trial of Probiotics in post-surgical colorectal cancer. *BMC Gastroenterol* 2019;19:131.
21 Liu Y, Lau HC-H, Yu J. Microbial metabolites in colorectal tumorigenesis and cancer therapy. *Gut Microbes* 2023;15:2203968.
22 Ting NL-N, Lau HC-H, Yu J. Cancer Pharmacomicrobiomics: targeting Microbiota to Optimise cancer therapy outcomes. *Gut* 2022;71:1412–25.
23 Beccari T. Lysosomal alpha-Mannosidase and alpha-Mannosidosis. *Front Biosci* 2017;22:157–67.
24 Cuskin F, Lowe EC, Temple MJ, *et al*. Human gut Bacteroidetes can utilize yeast Mannan through a selfish mechanism. *Nature* 2015;517:165–9.
25 Li Y, Li R, Yu H, *et al*. Enterococcus Faecalis Alpha1-2-Mannosidase (Efman-I): an efficient catalyst for glycoprotein N-Glycan modification. *FEBS Lett* 2020;594:439–51.
26 Kołaczkowski BM, Moroz OV, Blagova E, *et al*. Structural and functional characterization of a multi-domain Gh92 Alpha-1,2-Mannosidase from Neobacillus Novalis. *Acta Crystallogr D Struct Biol* 2023;79:387–400.
27 de Freitas Junior JCM, Morgado-Díaz JA. The role of N-Glycans in colorectal cancer progression: potential biomarkers and therapeutic applications. *Oncotarget* 2016;7:19395–413.
28 Zhao Q, Zhan T, Deng Z, *et al*. Glycan analysis of colorectal cancer samples reveals stage-dependent changes in CEA Glycosylation patterns. *Clin Proteomics* 2018;15:9.
29 Doherty M, Theodoratou E, Walsh I, *et al*. Plasma N-Glycans in colorectal cancer risk. *Sci Rep* 2018;8:8655.
30 He L, Fan C, Kapoor A, *et al*. Alpha-Mannosidase 2C1 attenuates PTEN function in prostate cancer cells. *Nat Commun* 2011;2:307.
31 Freeze HH, Kranz C. Endoglycosidase and Glycoamidase release of N-linked Glycans. *Curr Protoc Mol Biol* 2010;Chapter 17:Unit .

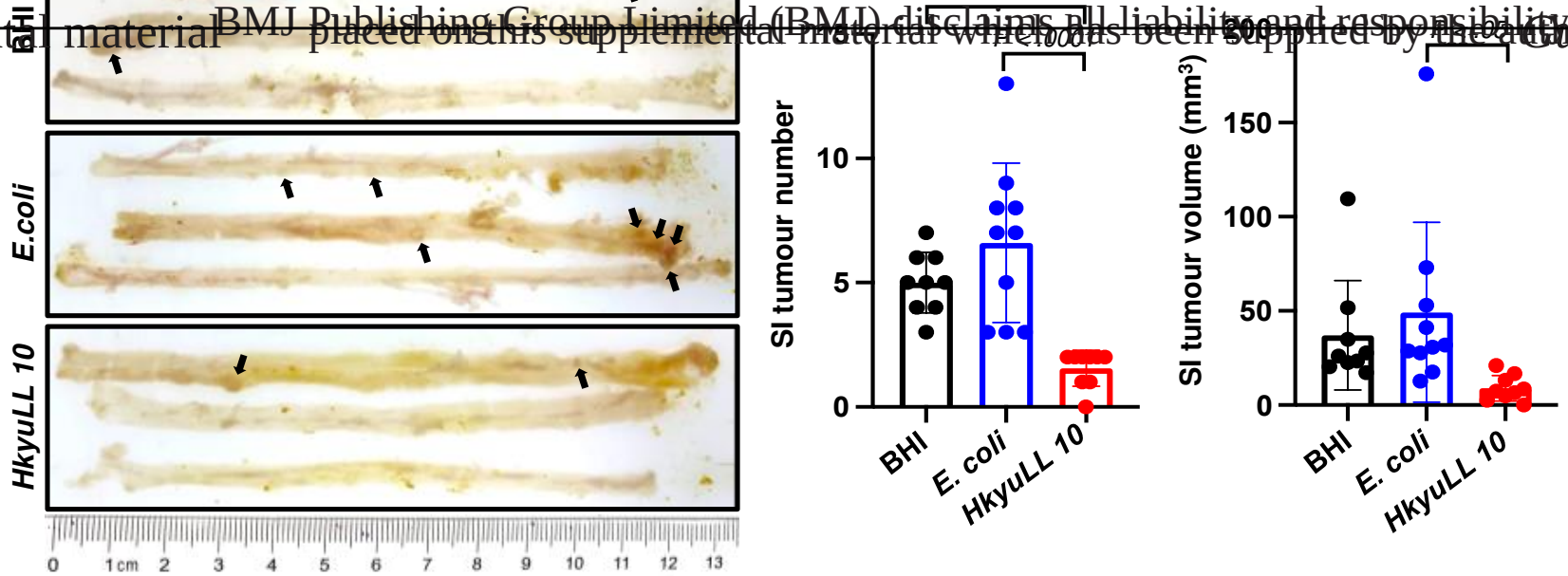

Supplementary Figure 1. Tumour formation in the small intestine of *Apc*$^{Min/+}$ mice. Small intestine morphology and tumour parameters, with black arrows indicating the visible tumours. SI, small intestine.

A ***Apc*$^{Min/+}$ mouse model

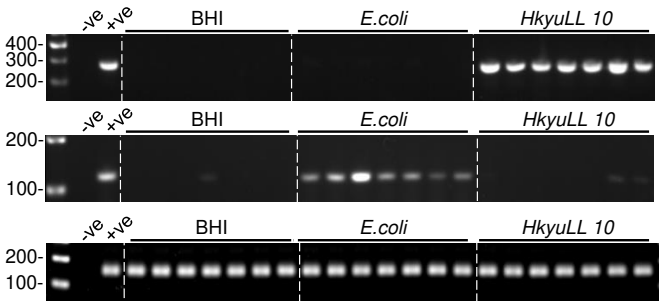

BLAST

Description	Scientific Name	Max Score	Total Score	Query Cover	E value	Per. ident	Acc. Len	Accession
Lactococcus lactis subsp. lactis strain UC08 plasmid pUC08A, complete sequence	*Lactococcus lactis* subsp. lactis	431	431	96%	4e-116	99.58	89016	CP016726.2

Description	Scientific Name	Max Score	Total Score	Query Cover	E value	Per. ident	Acc. Len	Accession
Escherichia coli strain K-12 chromosome, complete genome, complete genome	*Escherichia coli* str. K-12 substr. MG1655	141	141	98%	3e-34	96.51	4639694	CP032667.1

B **AOM/DSS mouse model**

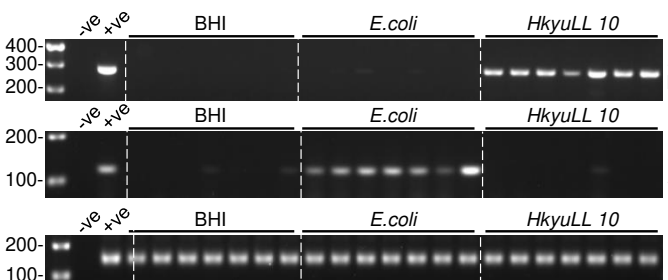

BLAST

Description	Scientific Name	Max Score	Total Score	Query Cover	E value	Per. ident	Acc. Len	Accession
Lactococcus lactis subsp. lactis strain UC08 plasmid pUC08A, complete sequence	*Lactococcus lactis* subsp. lactis	440	440	100%	7e-119	99.18	89016	CP016726.2

Description	Scientific Name	Max Score	Total Score	Query Cover	E value	Per. ident	Acc. Len	Accession
Escherichia coli strain K-12 chromosome, complete genome, complete genome	*Escherichia coli* str. K-12 substr. MG1655	141	141	86%	3e-34	96.51	4639694	CP032667.1

Supplementary Figure 2. Bacteria detection in gavaged mice. (A, B) DNA gel electrophoresis (left) and BLAST results from Sanger sequencing analysis (right) on faecal samples of *Apc*$^{Min/+}$ **(A)** or AOM/DSS-treated mice **(B)**.

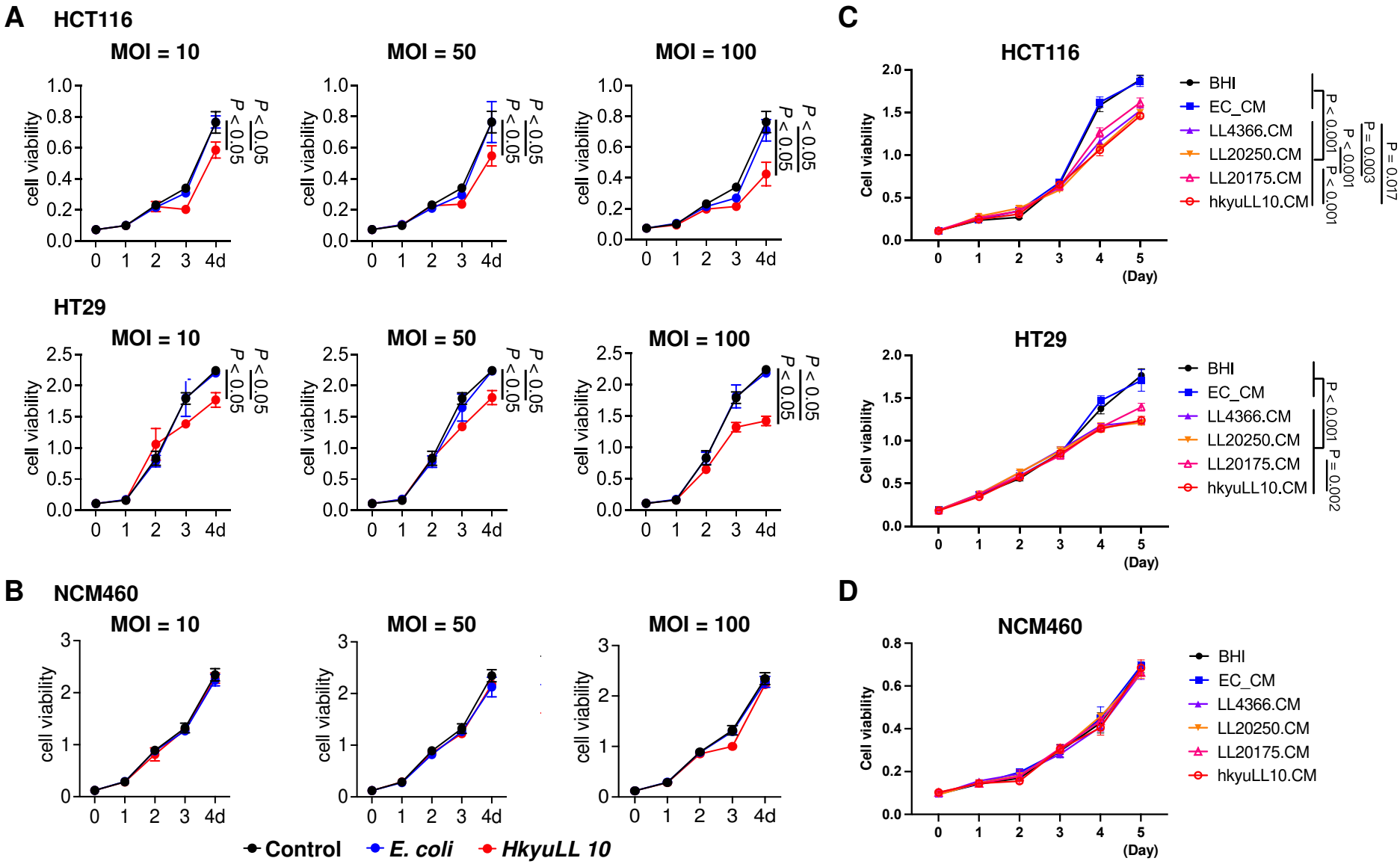

Supplementary Figure 3. *L. lactis* inhibits growth of CRC cells. (A, B) Cell viability at OD_{570} of human CRC cells (HCT116, HT29) **(A)** and normal colon epithelial cells (NCM460) **(B)** under treatment of direct bacteria culture at different multiplicity of infection. **(C, D)** Cell viability at OD_{570} of CRC cells **(C)** and normal cells **(D)** under treatment of 5% bacterial conditioned medium of different *L. lactis* strains. MOI, multiplicity of infection.

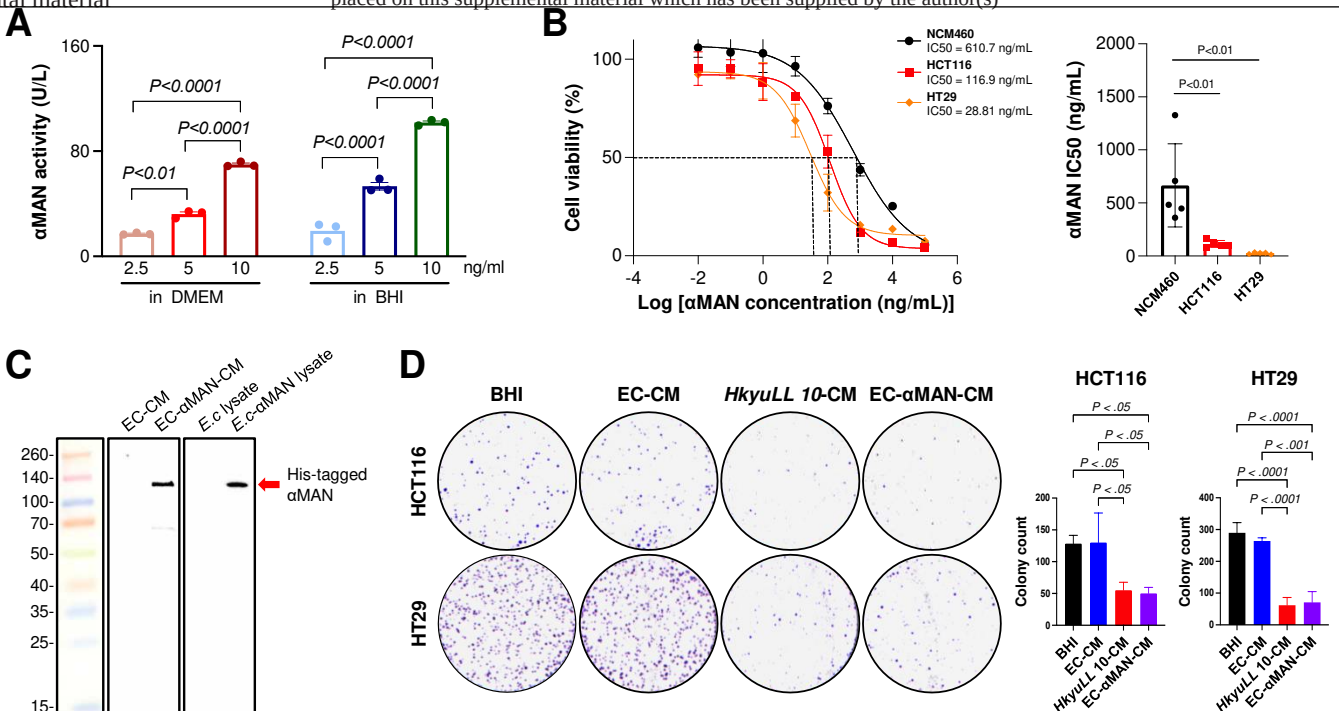

Supplementary Figure 4. Alpha-mannosidase inhibits growth of CRC cells. (A) Activity of αMAN in cell culture medium (DMEM) and bacteria culture broth (BHI). **(B)** IC50 of half-maximal inhibitory concentration of αMAN in CRC cells (HCT116, HT29) and normal cells (NCM460). **(C)** Construction of a mutant *E. coli* strain αMAN expression. αMAN was present in the conditioned medium and lysate of mutant but not wildtype *E. coli*. **(D)** Colony formation of CRC cells under treatment of 5% bacterial conditioned medium (> 100kDa). *E.c, E. coli*; EC-αMAN-CM, αMAN-expressing *E. coli* conditioned medium.

Supplementary Table 1. Primers for bacterial engineering of *E. coli* mutant strain with αMAN expression.

attλ-αMAN	Forward	CACCACCACCACCACCACTAAATACTAACTTGAGCGAAAC
	Reverse	GTACCGTTTTCTTTTTCATGGTATATCTCCTTCTTAAAGT
αMAN-attλ	Forward	TAAGAAGGAGATATACCATGAAAAAGAAAACGGTACATAT
	Reverse	GTGGTGGTGGTGGTGTTGATTTTTCTCCTTAATCAACAAA
αMAN-cx	Forward	TCGTTTTTAATACAGCTGGACA
	Reverse	TGATTTCAGCTGGCACTTCTTG
MG1655attλ	Forward	CACCCGGAGCGGCAGGGACATAT
	Reverse	CTGCTACGACCCGGATGCGCCAA

Supplementary Table 2. Primers for bacteria detection.

***Lactococcus lactis* HkyuLL 10**

	Sequence (5'->3')	**Template strand**	**Length**	**Start**	**Stop**	**Tm**	**GC%**
Forward primer	CCAGCCCATTGAACTTCCCT	Plus	20	218	237	59.96	55.00
Reverse primer	TCATCTGTTGTCCTCGCATTCT	Minus	22	502	481	59.77	45.45
Product length	285						

***Escherichia coli* MG1655**

	Sequence (5'->3')	**Template strand**	**Length**	**Start**	**Stop**	**Tm**	**GC%**
Forward primer	TCGCACTTTCCCTGGTTCTG	Plus	20	5259	5278	60.25	55.00
Reverse primer	ACCTCCATCCCAGTAATAGCCA	Minus	22	5380	5359	60.36	50.00
Product length	122						

Supplementary Table 3. Nano LC-MS analysis to characterize the five protein bands identified by silver staining.

Band	Position on gel (kDa)	Accession	Description	MW (kDa)	Sequest-HT score	Coverage (%)	Function
1	140-180	A0A2A9IP86	Glutamate synthase large subunit OS=Lactococcus lactis OX=1358 GN=BW154_06430 PE=3 SV=1	164.3	174.44	32	Pro-tumoural features
2	140-180	N/A	N/A	N/A	N/A	N/A	N/A
3	100-140	A0A2A9IKZ9	Valine--tRNA ligase OS=Lactococcus lactis OX=1358 GN=valS PE=3 SV=1	101	347.59	60	Loading valine onto its specific tRNA
		A0A2A9IP05	Endo-beta-N-acetylglucosaminidase OS=Lactococcus lactis OX=1358 GN=BW154_05500 PE=4 SV=1	102.3	317.81	56	Processing of free oligosaccharides in the cytosol
		A0A0V8DM88	Isoleucine--tRNA ligase OS=Lactococcus lactis subsp. lactis OX=1360 GN=ileS PE=3 SV=1	106.5	288.78	48	Catalysing the attachment of isoleucine to tRNA (Ile)
		A0A0V8CY66	Valine--tRNA ligase OS=Lactococcus lactis subsp. lactis OX=1360 GN=valS PE=3 SV=1	100.5	284.84	52	Loading valine onto its specific tRNA
		A0A2N5WA15	Cytosolic endo-beta-N-acetylglucosaminidase OS=Lactococcus lactis subsp. lactis OX=1360 GN=CYU10_002498 PE=4 SV=1	102.4	278.21	54	Processing of free oligosaccharides in the cytosol
		A0A0V8BFY1	Uncharacterized protein OS=Lactococcus lactis subsp. lactis OX=1360 GN=LKF24_2507 PE=4 SV=1	102.4	251.49	47	N/A

		A0A0V8DGH2	DNA-directed RNA polymerase subunit beta OS=Lactococcus lactis subsp. lactis OX=1360 GN=rpoB PE=3 SV=1	133.1	223.53	45	Polymerisation of ribonucleotides into complementary DNA
		A0A2A9IMI1	DNA-directed RNA polymerase subunit beta' OS=Lactococcus lactis OX=1358 GN=rpoC PE=3 SV=1	134.7	219.77	44	Polymerisation of ribonucleotides into complementary DNA
		D2BLI1	Isoleucine--tRNA ligase OS=Lactococcus lactis subsp. lactis (strain KF147) OX=684738 GN=ileS PE=3 SV=1	106.7	218.42	36	Catalysing the attachment of isoleucine to tRNA (Ile)
		A0A2A9INL0	**Alpha-mannosidase OS=Lactococcus lactis OX=1358 GN=BW154_05470 PE=3 SV=1**	**102.6**	**182.86**	**38**	**Alpha-mannosidase reduces high-mannose N-glycans, malignant progression markers in early-stage CRC**
		D2BKE9	**Alpha-mannosidase OS=Lactococcus lactis subsp. lactis (strain KF147) OX=684738 GN=ypdB PE=3 SV=1**	**102.1**	**167.28**	**36**	
		A0A2A9IR05	Pyruvate carboxylase OS=Lactococcus lactis OX=1358 GN=BW154_09950 PE=4 SV=1	126.5	143.83	35	Catalysing the HCO_3^-- and MgATP-dependent carboxylation of pyruvate to form oxaloacetate
4	100-140	A0A2A9IKZ9	Valine--tRNA ligase OS=Lactococcus lactis OX=1358 GN=valS PE=3 SV=1	101	490.21	67	Loading valine onto its specific tRNA
		A0A0V8CY66	Valine--tRNA ligase OS=Lactococcus lactis subsp. lactis OX=1360 GN=valS PE=3 SV=1	100.5	425.48	59	Loading valine onto its specific tRNA
		A0A2A9IMI1	DNA-directed RNA polymerase subunit beta' OS=Lactococcus lactis OX=1358 GN=rpoC PE=3 SV=1	134.7	333.97	57	Polymerisation of ribonucleotides into complementary DNA

		A0A0V8DGH2	DNA-directed RNA polymerase subunit beta OS=Lactococcus lactis subsp. lactis OX=1360 GN=rpoB PE=3 SV=1	133.1	274.3	55	Polymerisation of ribonucleotides into complementary DNA
		A0A7L9L7K3	Discoidin domain-containing protein OS=Lactococcus lactis OX=1358 GN=HZ322_06980 PE=4 SV=1	102.4	239.12	51	Blood coagulation factor
		A0A2A9IP05	Endo-beta-N-acetylglucosaminidase OS=Lactococcus lactis OX=1358 GN=BW154_05500 PE=4 SV=1	102.3	234.55	52	Processing of free oligosaccharides in the cytosol
		A0A2N5WA15	Cytosolic endo-beta-N-acetylglucosaminidase OS=Lactococcus lactis subsp. lactis OX=1360 GN=CYU10_002498 PE=4 SV=1	102.4	216.68	49	Processing of free oligosaccharides in the cytosol
		A0A0V8DM88	Isoleucine--tRNA ligase OS=Lactococcus lactis subsp. lactis OX=1360 GN=ileS PE=3 SV=1	106.5	216.63	46	Catalysing the attachment of isoleucine to tRNA (Ile)
5	100-140	A0A2A9IMI1	DNA-directed RNA polymerase subunit beta' OS=Lactococcus lactis OX=1358 GN=rpoC PE=3 SV=1	134.7	260.25	51	Polymerisation of ribonucleotides into complementary DNA
		A0A2A9IKZ9	Valine--tRNA ligase OS=Lactococcus lactis OX=1358 GN=valS PE=3 SV=1	101	240.33	48	Loading valine onto its specific tRNA
		A0A0V8DGH2	DNA-directed RNA polymerase subunit beta OS=Lactococcus lactis subsp. lactis OX=1360 GN=rpoB PE=3 SV=1	133.1	201.54	43	Polymerisation of ribonucleotides into complementary DNA

A0A0V8CY66	Valine--tRNA ligase OS=Lactococcus lactis subsp. lactis OX=1360 GN=valS PE=3 SV=1	100.5	195.46	42	Loading valine onto its specific tRNA
A0A2A9IP05	Endo-beta-N-acetylglucosaminidase OS=Lactococcus lactis OX=1358 GN=BW154_05500 PE=4 SV=1	102.3	135.45	37	Processing of free oligosaccharides in the cytosol
A0A0V8DM88	Isoleucine--tRNA ligase OS=Lactococcus lactis subsp. lactis OX=1360 GN=ileS PE=3 SV=1	106.5	129.92	36	Catalysing the attachment of isoleucine to tRNA (Ile)
A0A2N5WA15	Cytosolic endo-beta-N-acetylglucosaminidase OS=Lactococcus lactis subsp. lactis OX=1360 GN=CYU10_002498 PE=4 SV=1	102.4	119.31	35	Processing of free oligosaccharides in the cytosol

MW, molecular weight.

Supplementary Table 4. Sequence encoding α-mannosidase in *HkyuLL 10* genome.

Encoding sequence	atgaaaaagaaaacggtacatatcatctctcacagtcattgggatcgagaatggtatatggcttatgaagaacatcatatgcgtttagtcaattta gtggatgatttacttgatttattcaagaaagatcctgagtttgatagctttcatttggatggacaaacgattattttagatgactatttgcaagtacgtc ctgagcgtcgtgaggaagtacaagcagcggtttcagctggaaaattgaaaattggtccatttttatatcttacaagatgatttcctcattagttctga atcaaacgttcgtaatatgcttgttgggcgtaaagaatcggagcgttgggggctccagttgagttggggtatttccctgatacttttgggaatat gggccaaacgccacaaatgatgaaagcggcaggacttagcgctgcagcttttggtcgaggagtgaagccaatcgggtttgataatcaagtttt ggaacaatcagaggaagcctacagttcacaattttcagaaatgtggtgggaaggtcctgatgggacaaaaattcttggaattctatttgccaatt ggtattcaaatggaaatgaaattcctgctgaaaaagcagcagcacttgaattttggaatcaaaaattagcagatgttgaaaaatttgcttcgacat cacatctcttaatgatgaatggcgtggatcatcaaccagttcagaaagatttgagcaaagcgattcgcttggcaaatgaacttttcccagattatg agtttgttcattctaattggccaacttatttagaagctgtaaggtcagatttgtttgaaaacttatctacggtaacaggggaactaacctcacagga aactgatggctggtacactttagcaaatacggcttcgagtcgagtttatctcaaacaatggaatacaaaagttgagcgtcagttagaaaatgtta cagaacctctcgccagtttagcttatcgggtgacaggagagtatccgcacgacaaattgacttatgcttggaaaactttgatgcaaaatcatcca catgatagtatctgtggttgctctgttgacgaagttcatcgtgaaatgatgacacgttttgaaaaagcgaatgaagtagggaaatatcttgctgat gatgcattatttgaactcgctaaagtcattgactttgaaggccaacatccttttgtcgtttttaatacagctggacattctaaaacaggtgaggctga agttgaagtagttcttgagcgcaaattatttaaagaaggaattcctgaaaaactttatgatgaactaaaggcacagcccaaggcaacttataaag taatcaatcgtgaaggtcaagaagtgccagctgaaatcagtgaagaagaagttttatttgattatgatttaccgaaagatcgtttccgagttcctta catgaaacgatttgtgaaagtgaaattatttttaaatgaaatgagtgcttttcttgggaaagttttgatttggtacttactgacgatgctgacagcttt gataatagttctgtcagtaataatgaaagtatgatttctggtcaaacaattgaaaatgaaagtttgaaactgacagttaatcataatggaacattga gtatttttgataagtcgctcaataaagtttttaaagatttgcttgtctttgaagacactggtgatattggaaatgaatatatctatttccaacctaaaaat accaaagcaatttttttctactgacagtcctgttgaattttcaattattactgacagagcagaaattgcggaagttcagcttaaacaagtgctgatgat tcctgaatctgctgacgaattattggatgaggaacaaaaaaaaggttttggaattccgttatcgtaatgctggtcgttctgataaacttttgccttag aggtaacaagcaaaatcactgtacgtaaaaattcaaaaaaagttgattttgaaacaagcattgataatcaaatgaaagatcacagacttcgtgta ctattcccagcgggattaacaagcgaaaatcacgaagctgacagtatttatgaagtagtgacaagacctaatgttatgcctgaaacttgggaaa atccaacaaatccacagcatcagcaagctttcgttaatcttcacaatgaagaatatggtttaactgttggtaattttggtttaaatgaatatgaaatta ctgacagcgcaaatattgccctaactttacttagaggagttggagaacttggtgattggggttacttcccaacaccagaggctcaaactttagga cgtcatacttttaactatagtttagaatttcatggaccggcttacgaacgttatgaaacttatcaacatgcttatgttgcacaagttccatttttcaacg gtagaactgacaaatccgtcagcagaaaaaactttaccgtcagctgggagaatattagaaattgatactgataaatttgctatcacggcattgaa acgtcgcgaatcagataatggtctagttttacgaggctacaatatgtcntccggactttgttga
Amino acid sequence	MKKKTVHIISHSHWDREWYMAYEEHHMRLVNLVDDLLDLFKKDPEFDSFHLDGQTIILD DYLQVRPERREEVQAAVSAGKLKIGPFYILQDDFLISSESNVRNMLVGRKESERWGAPVE LGYFPDTFGNMGQTPQMMKAAGLSAAAFGRGVKPIGFDNQVLEQSEEAYSSQFSEMWW EGPDGTKILGILFANWYSNGNEIPAEKAAALEFWNQKLADVEKFASTSHLLMMNGVDH QPVQKDLSKAIRLANELFPDYEFVHSNWPTYLEAVRSDLFENLSTVTGELTSQETDGWYT LANTASSRVYLKQWNTKVERQLENVTEPLASLAYRVTGEYPHDKLTYAWKTLMQNHP HDSICGCSVDEVHREMMTRFEKANEVGKYLADDALFELAKVIDFEGQHPFVVFNTAGHS KTGEAEVEVVLERKLFKEGIPEKLYDELKAQPKATYKVINREGQEVPAEISEEEVLFDYD LPKDRFRVPYMKRFVKVKLFLNEMSAFSWESFDLVLTDDADSFDNSSVSNNESMISGQTI ENESLKLTVNHNGTLSIFDKSLNKVFKDLLVFEDTGDIGNEYIYFQPKNTKAIFSTDSPVEF SIITDRAEIAEVQLKQVLMIPESADELLDEEQKKVLEFRYRNAGRSDKLLPLEVTSKITVR KNSKKVDFETSIDNQMKDHRLRVLFPAGLTSENHEADSIYEVVTRPNVMPETWENPTNP QHQQAFVNLHNEEYGLTVGNFGLNEYEITDSANIALTLLRGVGELGDWGYFPTPEAQTL GRHTFNYSLEFHGPAYERYETYQHAYVAQVPFSTVELTNPSAEKTLPSAGRILEIDTDKFA ITALKRRESDNGLVLRGYNMXSGLC

SUPPLEMENTARY INFORMATION

Bacterial whole genome sequencing

High-quality genomic DNA extracted from bacteria culture was subjected to library preparation and whole genome sequencing using PacBio 3rd generation sequencing platform (Pacific Biosciences, Menlo Park, CA). Raw sequencing reads were filtered using circular consensus sequencing under default parameters (version 4.1). The filtered reads were then subjected to *de novo* genome assembly with Canu under default parameters, including read correction, read trimming, and contig construction. The quality of genome assembly was evaluated by CheckM. Genome annotation was performed by Rapid Annotation using Subsystem Technology (RAST).

Histological assessment

Paraffin-embedded colon tissues were sectioned (4 μm) and stained by haematoxylin and eosin staining. Histological assessment of tumours was evaluated by pathologists who were blinded to the group information. Images were captured by light microscope (Axio Imager 2, Zeiss, Jena, Germany) equipped with Metafer Automatic Slide Scanning and Imaging System (version 3.12.7; MetaSytems, Altlussheim, Germany).

Ki-67 immunohistochemical staining

Colon sections (4 μm) were deparaffinised, blocked, and incubated with anti-Ki-67 primary antibody (1:500; #ab16667, Abcam) at 4°C overnight. Signals were developed by IHC Select Immunoperoxidase Secondary Detection System (Merck) according to manufacturer's instructions. Haematoxylin was used for counterstaining, and rabbit serum diluted to the same concentration of

Su ACY, *et al. Gut* 2024;0:1–11. doi: 10.1136/gutjnl-2023-330835

primary antibody was used as negative control. Images were captured by light microscope equipped with Metafer Automatic Slide Scanning and Imaging System. The proportion of Ki-67 positive cells in each random field was measured by Image J with plugin IHC Profiler.

TUNEL staining

Colon sections (4 μm) were deparaffinised, rehydrated, and fixed in 4% paraformaldehyde for 15 minutes. 100 ml of proteinase K (20 mg/mL) was added to each slide and incubated at room temperature for 30 minutes. After PBS wash, slides were incubated with 100 mL of equilibration buffer at room temperature for 10 minutes, and with 100 mL of Tdt reaction mix at 37°C for 60 minutes. The reaction was stopped by 2X SSC and slides were blocked by 0.3% hydrogen peroxide for 5 minutes. 100 mL of streptavidin HRP (1:500 in PBS) was then added to slides and incubated at room temperature for 30 minutes. 100 mL of DAB solution was used to develop signals.

Bacteria detection

PCR was conducted on genomic DNA extracted from mouse stools using Premix Taq DNA Polymerase (Hot-Start Version; Takara, Kusatsu, Japan) in Veriti 96-Well Fast Thermal Cycler (Thermo Fisher Scientific, Rockford, IL). Each PCR mix contained 100 ng of sample DNA with a reaction volume of 10 μL. PCR cycle conditions are as follow: 1) 95°C for 5 minutes; 2) 95°C for 30 seconds, 57°C for 15 seconds, and 72°C for 30 seconds for 35-40 cycles; and 3) 72°C for 5 minutes. PCR products were subjected to agarose gel electrophoresis at 90V for 50 minutes, and captured by ChemiDoc XRS+ System (Bio-Rad, Hercules, CA). Primers used for bacteria detection are listed in **Supplementary Table 2**. A subset of PCR products was subjected to Sanger

sequencing performed by Sangon Biotech (Shanghai, China). The sequencing data were analysed using SnapGene Viewer (version 4.1) and BLAST (https://blast.ncbi.nlm.nih.gov/Blast.cgi).

Cell culture and CRC patient-derived organoid culture

Two human CRC cell lines HCT116 and HT29 as well as a human normal colon epithelial cell line NCM460, were purchased from American Type Culture Collection (Manassas, VA). Cells were cultured in Dulbecco's Modified Eagle's Medium (Gibco, Grand Island, NY) supplemented with 10% foetal bovine serum and 1% penicillin/streptomycin, and maintained at 37ºC in a humidified incubator with 5% carbon dioxide.

CRC organoids were derived from two CRC patients (#74 and #828) from Princess Margaret Living Biobank (Toronto, Canada), embedded into Matrigel (Corning), and cultured in DMEM/F12 (Gibco) with GlutaMAX (Invitrogen, Carlsbad, CA), N2 and B27 supplements (Invitrogen), 10 mmol/L HEPES, 1.25 mmol/L N-acetyl cysteine, glutamine, 1% penicillin/streptomycin, 10 mmol/L SB202190-monohydrochloride, R-spondin-1, Noggin, WNT3A, and 50 ng/mL epithelial growth factor (Invitrogen). Culture medium was changed every 3 days. After treatment of 7-10 days, images were captured and the surface area of organoids in each random field was measured by ImageJ (version 1.53a). The experiment was conducted with 9-12 organoids per group. To investigate candidate proteins, cells or organoids were directly treated with commercial αMAN (10 ng/mL in PBS; #M7257, Sigma-Aldrich). The activity of αMAN was determined using α-mannosidase Assay Kit (#ab272519, Abcam Cambridge, MA).

Cell viability and colony formation assays

Cell viability assay was performed using 3-(4,5-dimethylthiazol- 2-yl)-2,5-diphenyltetrazolium (MTT, 5 mg/mL; Invitrogen). 1,000 cells per well were seeded onto 96-well plates for treatment. Cell viability was determined by measuring absorbance at a wavelength of 570 nm (OD_{570}) to evaluate the amount of MTT formazan products for 4-5 consecutive days. The experiment was conducted with 5-10 replicates per group. For colony formation assay, 1,000 cells per well were seeded onto 6-well plates. Culture medium was changed every 3 days. After treatment of 10 days, colonies were fixed by ice-cold methanol and stained by 0.5% crystal violet. Colonies with more than 50 cells were captured and measured by ImageJ. The experiment was conducted with triplicates per group.

Ki-67 immunofluorescent staining

Cells were seeded onto coverslips in 4-well plates. After treatment of 4-5 days, cells were fixed by 4% formaldehyde in PBS and blocked by 1% bovine serum albumin. Cells were then incubated with anti-Ki-67 primary antibody (1:6400; #9449, Cell Signalling Technology, Danvers, MA) at 4°C overnight, followed by Alexa Fluor 488 secondary antibody (1:500; #A-11001, Thermo Fisher Scientific) at room temperature for 60 minutes in dark. Cells were mounted with 5-minutes nuclear counterstaining by DAPI solution (1 mg/mL; Thermo Fisher Scientific). Images were captured by confocal microscope. The proportion of Ki-67 positive cells in each random field was measured by ImageJ with plugin IHC Profiler. The experiment was conducted with triplicates per group.

Bacteria attachment assay

Cells were seeded onto 24-well plates at ≥ 90% of coverage and cell count was recorded. Bacteria culture at growth phase (OD_{600} = 1) was centrifuged and collected after PBS wash. The obtained bacteria were then added to each well (multiplicity of infection = 10, 50, 100), and incubated with cells at 37ºC for 3 hours. After PBS wash, cells were decomposed by adding 400 μL of BHI broth and 100 μL of bacteria-free double-distilled water. Serial dilutions (1:1, 1:10, 1:100, 1:1000) were prepared for all samples and controls. 100 μL of diluted solutions was spread onto BHI agar plate and incubated at 37ºC overnight. Colony-forming unit was recorded to determine the ratio of bacteria-cell attachment. The experiment was conducted with triplicates per group.

Protein extraction and Western blot

Total proteins were extracted from human CRC cell lines (HCT116, HT29) by CytoBuster Protein Extraction Reagent (Merck) supplemented with protease inhibitor and phosphatase inhibitor. Sample mixtures were incubated at 4ºC for 60 minutes. Supernatants were collected upon centrifugation at 16,000 ×g, 4ºC for 10 minutes. Protein concentration was measured by Pierce BCA Protein Assay Kit (Thermo Fisher Scientific) according to manufacturer's instructions. 20-40 mg of the extracted proteins were separated by 10% SDS-PAGE gel electrophoresis and transferred onto PVDF membranes with pore size of 0.22 or 0.45 μm (Merck). Membranes were then blocked by 5% bovine serum albumin for 60 minutes, and incubated with primary anti-PCNA antibody (1:2000; #2586, Cell Signalling Technology) at 4°C overnight, followed by 60-minutes incubation of anti-mouse IgG, HRP-linked secondary antibody (1:10,000; #7476, Cell Signalling Technology) at room temperature. After substantial wash by detergent (Tris-buffered saline with

Su ACY, *et al. Gut* 2024;0:1–11. doi: 10.1136/gutjnl-2023-330835

0.1% Tween-20), proteins of interest were visualised by Clarity Wstern ECL Substrate (Bio-Rad) using ChemiDoc XRS+ System. β-actin was used as the housekeeping control.

Silver staining

Proteins were resolved by 5% SDS-PAGE and silver staining was performed according to manufacturer's instructions (Thermo Fisher Scientific). In brief, visually intense bands at 100kDa fraction were collected for in-gel digestion and decolourisation. Gel pieces were incubated with 800 µL of ACT for 10 minutes, 600 µL of 5mM DTT at 55°C for 30 minutes, and 800 µL of ACN for 10 minutes. Gels were then alkylated by 600 µL of 15mM IAA for 40 minutes in dark, followed by digestion using 600 µL of trypsin buffer at 37ºC for 30 minutes. The digested peptides were isolated by 800 µL of extraction buffer, vacuum dried, and resuspended in 0.1% formic acid for liquid chromatography-mass spectrometry.

Nano LC-MS and analysis

5 mL of total peptides were subjected to nanoflow ultra-performance LC-MS instrument (EASY-nLC1200) coupled to Q Extractive HF-X Quadrupole-Orbitrap MS System (Thermo Fisher Scientific). Separation was performed using reversed phase column (100 mm ID x 15 cm, Reprosil-Pur 120 C18-AQ, 1.9 mm; Dr. Maisch, Ammerbuch, Germany) under two mobile phases (phase A, H_2O with 0.1% formic acid, 2% acetonitrile; phase B, 80% acetonitrile, 0.1% formic acid) with a 60-minute gradient at a flow rate of 300 nL/min. Data-dependent acquisition was conducted at a resolution of 120,000 (200 m/z) and m/z range of 350-1600 for MS1; and at a resolution of 15,000 with dynamic first mass for MS2. The automatic gain control target for MS1

was 3e6 with maximum injection time of 50 milliseconds; and 1e5 for MS2 with maximum injection time of 110 milliseconds. The top 10 most intense ions were fragmented at normalised collision energy of 27% and isolation window of 1.2 m/z. The dynamic exclusion time window was 45 seconds, and peaks with charge > 6 were excluded. Candidate proteins were screened by the following criteria: (1) matching molecular weight corresponding to the position of protein bands on SDS-PAGE gel after silver staining (100-140kDa or 140-180kDa); and (2) molecular weight > 100kDa, Sequest-HT score > 100, coverage > 30%.